

**DESIGN AND SYNTHESIS OF MOLECULAR RESISTS FOR HIGH
RESOLUTION PATTERNING PERFORMANCE**

A Thesis
Presented to
The Academic Faculty

by

Ameneh Cheshmehkani

In Partial Fulfillment
of the Requirements for the Degree
Master of Science in the
School of Chemistry & Biochemistry

Georgia Institute of Technology
December 2013

COPYRIGHT 2013 BY AMENEH CHESHMEHKANI

**DESIGN AND SYNTHESIS OF MOLECULAR RESISTS FOR HIGH
RESOLUTION PATTERNING PERFORMANCE**

Approved by:

Dr. Clifford L. Henderson, Advisor
School of Chemical and Biomolecular
Engineering
Georgia Institute of Technology

Dr. John R. Reynolds
School of Chemistry & Biochemistry
Georgia Institute of Technology

Dr. Dennis W. Hess
School of Chemical & Biomolecular
Engineering
Georgia Institute of Technology

Dr. Laren Tolbert, Advisor
School of Chemistry & Biochemistry
Georgia Institute of Technology

Dr. David Collard
School of Chemistry & Biochemistry
Georgia Institute of Technology

Date Approved: August 9, 2013

This thesis is dedicated to my husband Mohamad Hadi, and my daughter Fatemeh Saba

ACKNOWLEDGEMENTS

I would like to thank my research advisors (Prof. Tolbert and Prof. Henderson) for their advice, support and guidance during my research study. Their constructive interactions with me at every stage of my research made me a better thinker and researcher and I thank them for giving me the opportunity to be in their respected groups. I would also like to thank Prof. John Reynolds, Prof. Dennis Hess, and Prof. David Collard for serving on my committee. I would like to thank the members of Prof. Henderson and Prof. Tolbert groups that helped me a lot and generously assisted me every time that I had a question. I especially thank Dr. Richard Lawson, Nathan Jarnagin, Dr. Jing Cheng and Dr. Janusz Kowalik.

I would really like to thank my mother Mahnaz Mosaddeghi that helped me from when I was a child until now. I do appreciate it that she took care of my baby when I really needed her help. I would like to thank my father Hashem Cheshmehkani. He always tells me that I should rely on myself in every situation, and if I fall down, I have to stand up and start stronger than before. I would like to thank my sisters and brother, which are source of joy in my life. I would really want to thank my dearest husband Dr. Mohamad H. Kassae that helps me very much and supports me in every situation. He is the love of my life, my soul, and my happiness in the world. He means everything to me.

TABLE OF CONTENTS

ACKNOWLEDGEMENTS	IV
LIST OF FIGURES	VIII
SUMMARY	XI
CHAPTER 1 - INTRODUCTION TO LITHOGRAPHY AND PHOTORESISTS... 1	
1.1 Overview.....	1
1.2 Exposure Source	4
1.3 LER and Resolution.....	6
1.4 Chemically-Amplified (CA) and None chemically-Amplified Resists	7
1.5 Molecular Glass	10
1.6 Molecular Design.....	15
1.7 References.....	17
CHAPTER 2 -ACRYLATE-BASED RESISTS AND STUDYING PATTERNING	
PERFORMANCE	21
2.1 Introduction.....	21
2.2 Thermal Curing Procedure.....	23
2.3 Materials and Instruments.....	24
2.4 BHPF (9,9-bis(4-hydroxyphenyl)fluorene)	24
2.4.1 Synthesis of BHPF-2MA	26
2.4.2 Thermal Curing of BHPF-2MA.....	27
2.5 Thermal Curing of Trimethylolpropane Triacrylate (TMPTA).....	28
2.6 Relationship between Structure and Property	30

2.7 Thermal Curing of BPF-2A	31
2.8 Thermal Curing of BPA-G-2MA.....	32
2.9 Auto Thermal Polymerization Characterization	33
2.10 Positive tone Cross-Linking.....	34
2.10.1 Synthesis of Hex-2MA	35
2.11 Conclusion	37
2.12 References.....	39
CHAPTER 3-SYNTHESIS AND CHARACTERIZATION OF	
CALIX[4]RESORCINARENE AND ITS DERIVATIVES	42
3.1 Introduction.....	42
3.1.1 Calixarene Structure.....	43
3.1.2 Nomenclature	44
3.1.3 Calixarene Conformers	46
3.2 Cationic Polymerization	50
3.3 Materials and Instruments.....	52
3.4 Synthesis of Calix[4]resorcinarenes (C4MR).....	52
3.5 Synthesis and Characterized Fully Functionalized C4MR	54
3.5.1 Synthesis of C4MR-8Ox.....	55
3.5.2 Synthesis of C4MR-8Allyl	56
3.5.3 Synthesis of C4MR-8Ep	64
3.6 Conclusion	68
3.7 References.....	69
CHAPTER 4-SUMMARY AND FUTURE WORK	71

4.1 Summary.....	71
4.2 Future Work.....	72
4.2.1 Preliminary Result	73
4.3 References.....	75

LIST OF FIGURES

Figure 1.1. Moore's Law.....	2
Figure 1.2. Photolithography Process	3
Figure 1.3. Effect of LER on Patterning	6
Figure 1.4 Typical components of CAR and non-CAR resists.....	8
Figure 1.5. Solubility change of CAR resist with acid reaction (a), lithography procedure for CAR resists (b)	9
Figure 1.6 Mechanism for non-CAR resists inhibitors	10
Figure 1.7 Examples of molecular resists	11
Figure 1.8 Size comparison between a typical polymer resist and a typical molecular glass.....	12
Figure 1.9. Volume comparisons between polymer resist and molecular glass	14
Figure 2.1. Radical polymerization of acrylates	22
Figure 2.2. Chemical Structure of solvents used in thermal curing procedure	24
Figure 2.3. Structures of 9,9-bis(4-hydroxyphenyl)fluorene (BHPF)	25
Figure 2.4. Synthesis of BHPF-2MA.....	26
Figure 2.5. Structure of BHPF-2MA (a), NRT as a function of temperature in MIBK or MeOH (b). Normalized thickness to unwashed thickness of 70°C (c)	27
Figure 2.6. TMPTA structure (a), and NRT as a function of temperature (b).....	29
Figure 2.7. Chemical structure of BPA-2MA, BPA-G-2MA, and BPF-2A.....	31
Figure 2.8. BPF-2A structure and NRT as a function of temperature for BPF-2A film..	32
Figure 2.9. Structures of BPA-G-2MA and BPF-2A (a), and NRT as a function of temperature for BPA-G-2MA, and BPF-2A films (b)	33

Figure 2.10. NRT as a function of temperature for BPA-G-2MA, with and without initiator (AIBN) at 130°C	34
Figure 2.11. Process for developing positive tone photoresist	35
Figure 2.12. Structure of Hex-2MA (a), and synthesis reaction for Hex-2MA (b)	36
Figure 3.1. Calixarene compound with OH groups in intraannular (“endo-annular”) position (a), and in extraannular (“exo-annular”) position (b).....	44
Figure 3.2. Space-filing molecular model of a calixarene compound (left) and a vase (right)	44
Figure 3.3. Different calixarene compounds: calix[4]arene (a), calix [5]arene (b), calix [6]arene (c), and calix [8]arene (d)	45
Figure 3.4. Five different conformers of calix[4]arenes based on ring orientation	46
Figure 3.5. Four different conformers of calix[4]arenes (and calix[4]resorcinarene) based on substituents at the methylene bridges	47
Figure 3.6. Crown conformer structure that has the maximum hydrogen bonding among conformers	48
Figure 3.7. Boat and crown conformer conversions for calix[4]resorcinarene	48
Figure 3.8. Concentration of calix[4]resorcinarenes conformers as a function of time, in 5% solution of HCl in methanol at 50°C	49
Figure 3.9. Cationic polymerization of epoxy and oxetane	51
Figure 3.10. Synthesis route for making C4MR	52
Figure 3.11. Mechanism for synthesizing of C4MR.....	53
Figure 3.12. Mechanism of phase-transfer catalysis.....	55
Figure 3.13. Synthesis reaction of C4MR-8Ox.....	55

Figure 3.14. Synthesis reaction of C4MR-8Allyl	56
Figure 3.15. ¹ H-NMR (400 MHz) spectra of C4MR-8Allyl in CDCl ₃ at room temperature.	57
Figure 3.16. Common conformers of calix[4]resorcinarene	58
Figure 3.17. ¹ H-NMR (400 MHz) spectra of C4MR-8Allyl in CDCl ₃ at 45, 55, and 65°C	59
Figure 3.18. ¹ H-NMR (400 MHz) spectra of C4MR-8Allyl in CDCl ₃ at -70,-46, and -23°C	59
Figure 3.19. ¹ H- ¹ H COSY NMR spectrum of C4MR-8Allyl in CDCl ₃ at -70°C and peak assignment.....	61
Figure 3.20. ¹ H-NMR for C4MR-8Allyl at different temperatures	62
Figure 3.21. Catalytic epoxidation of C4MR-8Allyl with oxone for C4MR-8Ep synthesis	64
Figure 3.22. Reaction mechanism of epoxidation of carbon-carbon double bond	65
Figure 3.23. Reaction synthesis of C4MR-8Ep by functionalizing C4MR using epibromohydrine.	66
Figure 4.1. Structures of C4MR and full functionalized C4MR with oxetane (Ox), allyl, and epoxy (Ep).....	72

SUMMARY

In this thesis, different approaches in synthesizing molecular resist are examined, and structure-property relations for the molecular resist properties are studied. This allows for design of resists that could be studied further as either negative or positive tone resists in photolithography. A series of compounds having different number of acrylate moiety, and different backbones were investigated for photoresist application. Thermal curing of acrylate compounds in organic solvent was also examined. Film shrinkage, as well as auto-polymerization was observed for these compounds that make them unsuitable as photoresist material. Furthermore, calix[4]resorcinarenes (C4MR) was chosen as backbone, and the functional groups was selected as oxetane and epoxy. Full functionalized C4MR compounds with oxetane, epoxy and allyl were synthesized. Variable-temperature NMR of C4MR-8Allyl was studied in order to get a better understanding of the structure's conformers. Energy barrier of exchange (ΔG^\ddagger) was determined from coalescence temperatures, and was 57.4 KJ/mol for aromatic and vinyl hydrogens and 62.1 KJ/mol for allylic hydrogens.

CHAPTER 1 - INTRODUCTION TO LITHOGRAPHY AND PHOTORESISTS

1.1 Overview

Lithography is the process of transferring an image on a substrate. The origin of the word lithography comes from the Greek *lithos*, meaning stones, and *graphia*, meaning to write, so it means writing on stones. One of the mostly used lithography method is photolithography. Photolithography is mainly used to produce pattern on semiconductor devices during the production of integrated circuit (IC). Microelectronic devices based on integrated circuits (ICs) are embedded in systems such as automobile, industrial control, televisions, office equipment, games, toys, and in telecommunication equipment. The goal in fabrication of electronic devices is making smaller sized integrated circuits. However, production of smaller sized ICs causes a rise in price of an IC due to requiring more investment in expensive equipment for ICs systems¹. By using microelectronics in ICs, not only computing power will increase over time, but also the cost for this kind of device will decrease. In 1960s, Electronics Magazine published a paper in which Gordon Moore made a prediction about the semiconductor industry². This prediction is now known as Moore's law. He stated that the integrated circuit capacities will be doubling every 18 to 24 months³⁻⁵. This trend is shown graphically in Figure 1.1.

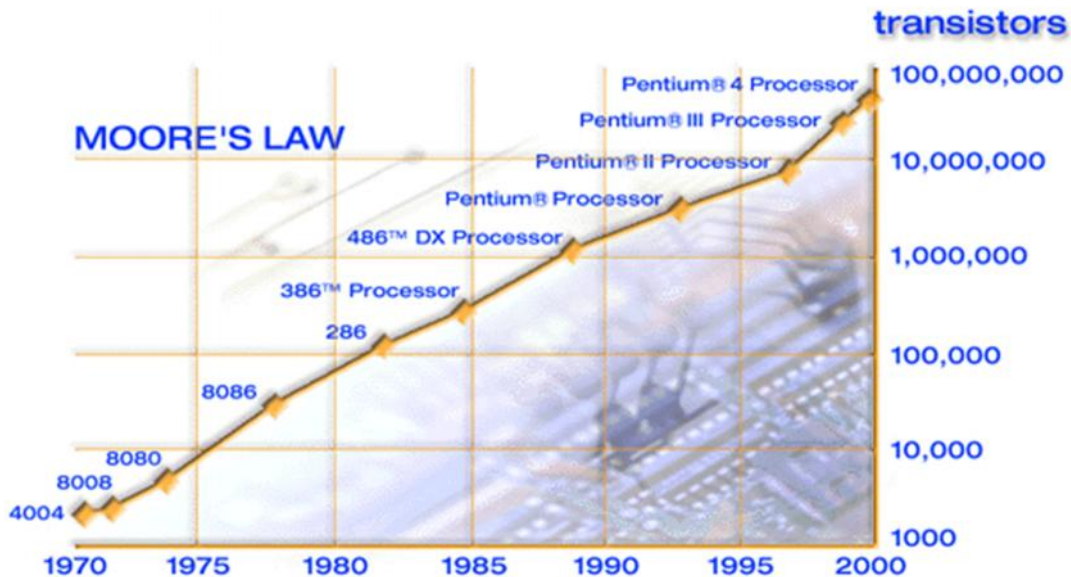


Figure 1.1. Moore's Law⁴

Photolithography uses light to generate the patterns. It is a process by which a light sensitive polymer, called a photoresist, is exposed to light and developed to form relief images on a substrate⁶.

Figure 1.2 shows a typical photolithography process. A thin film of a light sensitive material is deposited on a silicon wafer via spin-coating. The photoresist layer is exposed to a source of activating radiation (light) through a photomask. Depending on the desired pattern, photomask has areas that are opaque to activating radiation and other areas that are transparent to radiation. Light exposure transfers the pattern of the photomask to the photoresist-coated substrate. Following radiation exposure, the photoresist is developed to provide a relief image that permits selective processing of the substrate. The substrate processing depends on the type of the photoresist used in the lithography.

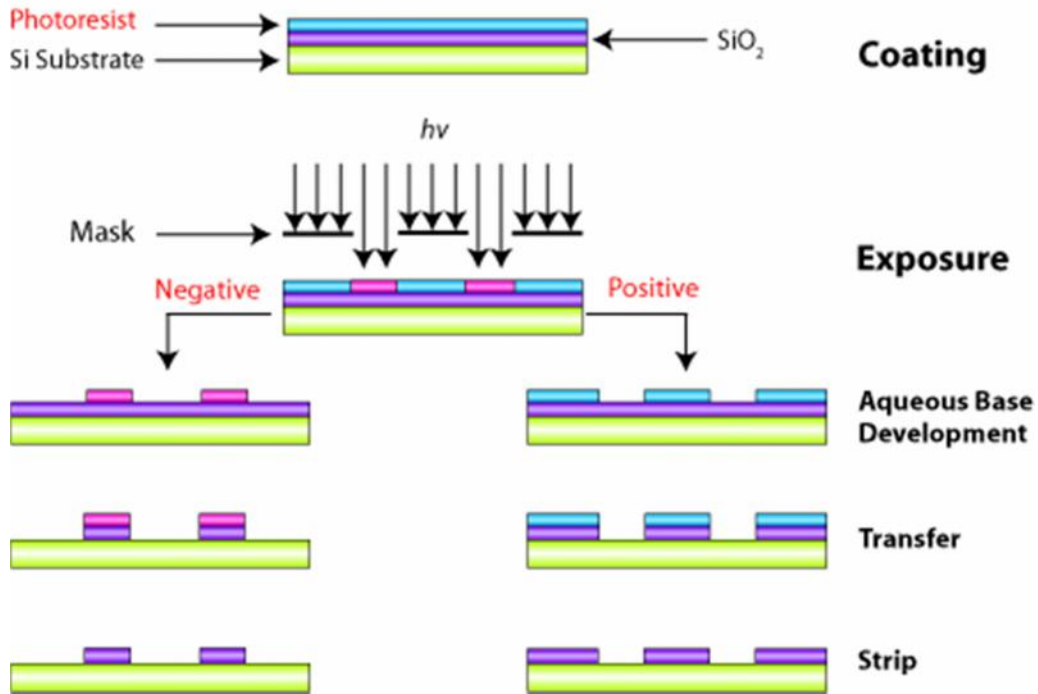


Figure 1.2. Photolithography Process

Photoresist material can be either positive tone or negative tone. The main difference in these two types of resists is their different solubility characteristics in exposed and unexposed areas. In using positive photoresists, UV light strategically hits the layer in areas that are intended for removal. When the photoresist is exposed to UV light, its chemical structure changes and becomes more soluble in the photoresist developer solvent. These exposed areas are then washed away with the solvent, with the unexposed areas remaining on the substrate due to not being soluble to the photoresist developer. Therefore, an identical copy of the mask's pattern is produced by using positive photoresists. Positive tone resists are, by far, the most common resist type used in high volume integrated circuit manufacturing. They are characterized by their excellent

resolution capabilities, especially in modern chemically amplified resists, and their facile processing by using aqueous developers.

Contrary to positive tone resists, the UV exposed areas become insoluble to the developer solvent in negative tone resists. The unexposed areas would be washed away by the developer solvent. Negative tone resists have, over the years, gained a somewhat less favorable reputation due to the perception that swelling during development can impose resolution limitations⁷. They also require organic solvents instead of aqueous solutions for development, and in some cases, suffer from relatively poorer etch resistance^{7,8}. However, negative polymeric resists are used in high volume integrated circuit manufacturing for certain device levels, and in applications where the cross linked nature of the negative systems is an advantage.

1.2 Exposure Source

In photolithography, a radiation source (exposure source) is used to transfer the pattern to substrate. There are several exposure sources used in lithography such as ultraviolet (UV)⁹⁻¹², deep ultraviolet (DUV)¹³⁻¹⁵, e-beam¹⁶⁻¹⁸, and extreme ultraviolet (EUV)¹⁹⁻²¹. In UV lithography, high pressure mercury (Hg) arc lamp is used as exposure source. In this lamp, the three main wavelengths are G-line (436 nm), H-line (405 nm), and I-line (365 nm). The light from the lamp is collected by a series of lenses and is focused onto the mask. There are also other lenses in the instrument that collect diffracted light from open areas of the mask, and focus it onto the photoresist layer.

Deep ultraviolet (DUV) lithography is another exposure source that uses Hg-Xe arc lamp. The most important DUV wavelengths are 248 nm, and 193 nm. KrF excimer laser produces 248 nm wavelength, and an ArF excimer laser produces 193 nm

wavelength. The procedure is similar to UV lithography. In this exposure, a series of quartz lenses conduct light to the mask and then to photoresist, which could generate three dimensional relief images.

Electron beam lithography (e-beam lithography) is the process of emitting focused beam of electrons on photoresist film to make pattern^{22,23}. This technique was developed for manufacturing integrated circuits, and for creating nanotechnology architectures. A tungsten thermionic emission cathode is often used in an electron gun²⁴. Both electrostatic and magnetic lenses may be used. Beam deflection coils are used for focusing the beam in a patterned fashion. The spot size can be less than 10 nm in diameter. E-beam lithography does not need mask because lenses and deflectors allow very fine control of the spot location. The key limitation of e-beam lithography is the very long time it takes to expose an entire silicon wafer or glass substrate. It can take several hours to expose a single wafer; or for some complex patterns it can take days to completely pattern. This is an important drawback for this system, because in standard optical lithography, the process of patterning on silicon wafer can be much faster²⁵.

Extreme ultraviolet (EUV) lithography is considered to be a key for next-generation lithography (NGL). Irradiation at 13.4 nm would be utilized for production of feature sizes less than 30 nm²⁶. When pattern size decreases, the key limitations of polymeric materials due to their large molecular size may become more serious²⁶⁻²⁹. The typical size of macromolecule compounds is in the range of several nanometers depending on chemical structure and molecular weight of the photoresist. However, for next generation lithography this typical polymer size is very close to the patterning

dimension²⁶. This technique has wavelength radiation from 365 to 248 nm, and more recently it goes down to 193 nm, to achieve higher resolution²⁶.

1.3 LER and Resolution

In design and manufacture of semiconductors, in order to increase processor speed, most of the focus is on producing a smaller feature size³⁰⁻³². Photoresist performance in making smaller future size is limited significantly by some factors such as line edge roughness (LER), and resolution.

Line edge roughness (LER) refers to fluctuations that happen on the edges of patterned lines. Recently, LER has received a lot of attention because it has been shown that it has negative effect on device performance^{33,34}. Studies have shown that LER and feature size does move parallel and it makes more serious issue for next generation lithography because the goal is small features²⁶. LER is affected by many factors such as shot noise³⁵ mask imperfection, acid diffusion³⁶ resist structure³⁷, and processing conditions³⁸. Figure 1.3 shows the effect of LER on patterning.

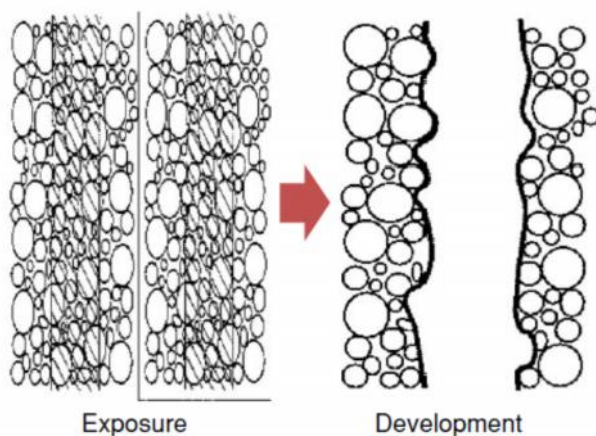


Figure 1.3. Effect of LER on Patterning³⁹

Resolution refers to the minimum feature size that can be relieved on the surface of the wafer with high reliability to a resist film⁴⁰. There is a quantitative measurement for relationship between contribution of photoresist and optics improvements that can be obtained by using Rayleigh's equation^{40,41},

$$\text{Resolution} = k_1 \frac{\lambda}{\text{NA}}$$

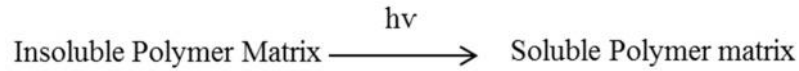
Where λ is the exposure wavelength, NA is the numerical aperture of the exposure tool, and k_1 factor is a collection of optical effects, properties of resist, and resist process⁴¹.

1.4 Chemically-Amplified (CA) and None chemically-Amplified Resists

The majority of resists used in semiconductor production now have multicomponent in their formulations. In general, these multicomponent resists can be classified as either chemically-amplified resists (CAR) or non-chemically amplified resists (non-CAR). Figure 1.4 shows typical compounds in CAR and non-CAR resists⁴².

Non-Chemically Amplified Resist

Novolac /DNQ Type Resist



Chemically Amplified Resist

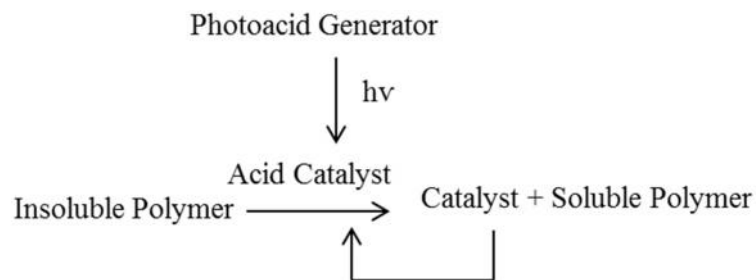


Figure 1.4. Typical components of CAR and non-CAR resists⁴²

Most commercial photoresists currently used in lithography are chemically amplified resists (CARs)⁴³. There are four general components in typical CAR formulations: polymer, photoacid generator (PAG), base, and solvent. When photoresist film is exposed to light, PAG is decomposed and forms a strong acid. The polymer contains functional groups, which are labile to acid and react in acidic environment to form polar compounds. The polarity of photoresist film increases in the exposed regions, these regions become soluble in aqueous base. The pattern can be developed by immersion in aqueous alkaline solution or in appropriate solvent. Figure 1.5 shows the procedure is using CAR resists⁴⁴.

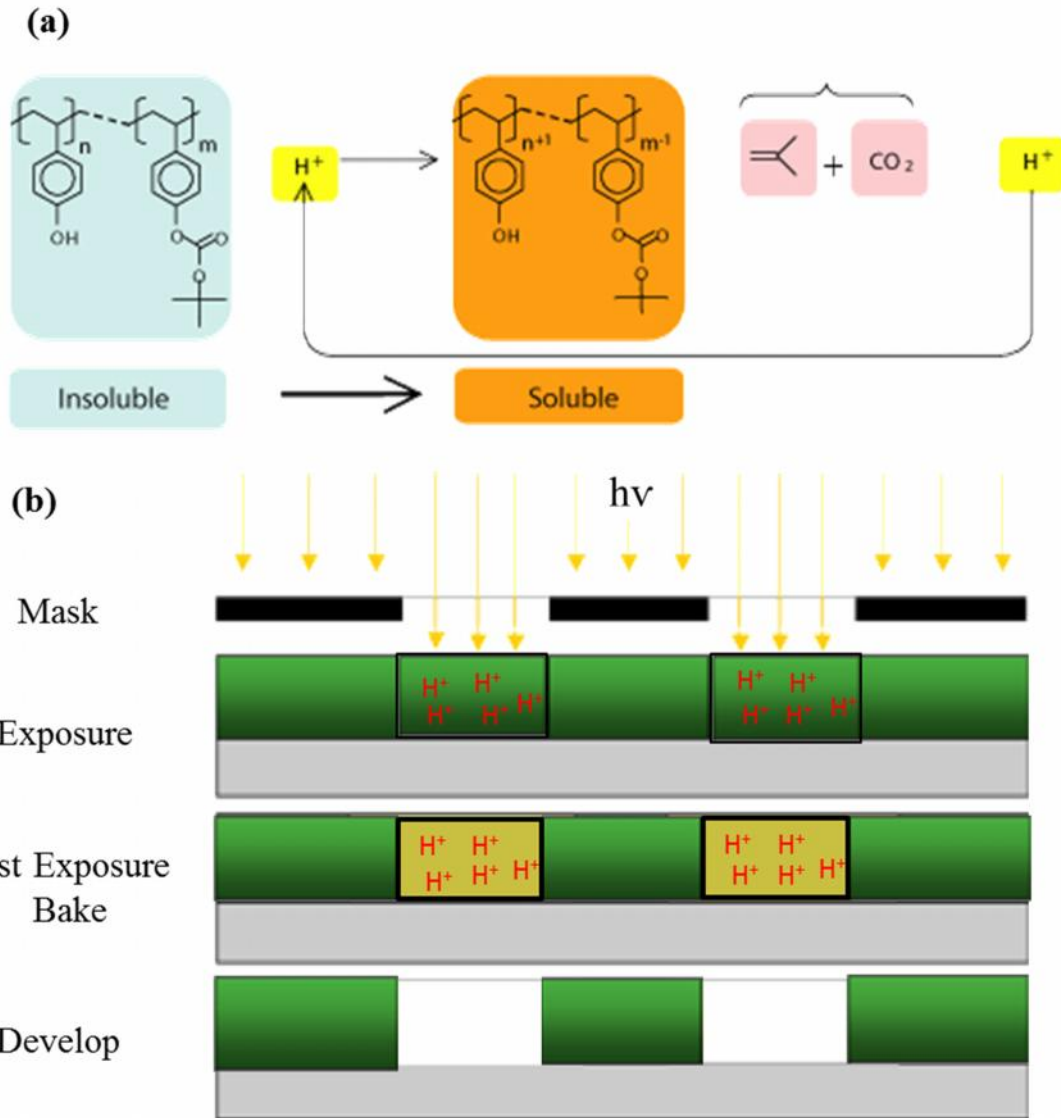


Figure 1.5. Solubility change of CAR resist with acid reaction (a), lithography procedure for CAR resists (b)⁴⁵

Non-chemically amplified resist (non-CAR) usually consist of only two components: polymer and solvent. There are two mechanisms for patterning with non-CARs resists. The first mechanism is chain scission. In this type of resists, polymer directly absorbs photons, which induces polymer backbone scissions, thereby increasing polymer solubility⁴³. The second mechanism utilizes photoactive dissolution inhibitors.

They convert into having base soluble group upon exposure to radiation, like diazonaphthoquinone⁴⁶. Figure 1.6 shows the second mechanism for non-CAR resists⁴⁷.

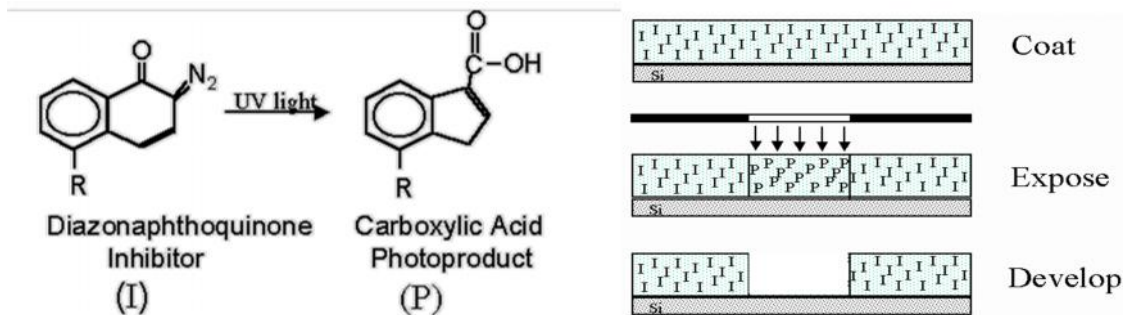


Figure 1.6. Mechanism for non-CAR resists inhibitors⁴⁷

1.5 Molecular Glass

As the semiconductor industry moves to smaller feature sizes, line edge roughness (LER) becomes a major issue^{48,49}. Different investigations have shown that limitations on resolution and LER are dependent on both the process and material⁵⁰. Size of the resist is an important factor in determining resolution features. The large size of polymer resists (~ 5 - 10 nm) create a huge limitation for achieving high resolution in photolithography⁵¹. These drawbacks have encouraged researchers to look for alternative resist materials. Therefore, new lithographic technologies and photoresist materials are being developed to overcome these limitations and satisfy the growing demand for higher resolution. Molecular glass resists (MG) are another group of compounds in family of resists that have been developed to improve lithography performance.

Molecular glass resists (MG) are low molecular weight organic photoresist materials that make stable amorphous glasses above room temperature. Molecular glasses were first used as photoresists in 1995 by Fujita *et. al*⁵². These functional materials have received great attention in optoelectronic devices and nanolithography⁵³⁻⁵⁵. Structural

features of molecular glasses prevent crystallization and increase high glass transition temperatures (T_g) despite their modest size. Therefore, these materials have recently produced extensive interest in organic electronics⁵⁶, and more recently as novel photoresists⁵⁷. Common glass forming topologies include branched, star shaped^{58,59}, twin molecular structures^{60,61}, tetrahedral^{62,63}, and spiro links⁶⁴. Figure 1.7 shows some examples of molecular resists.

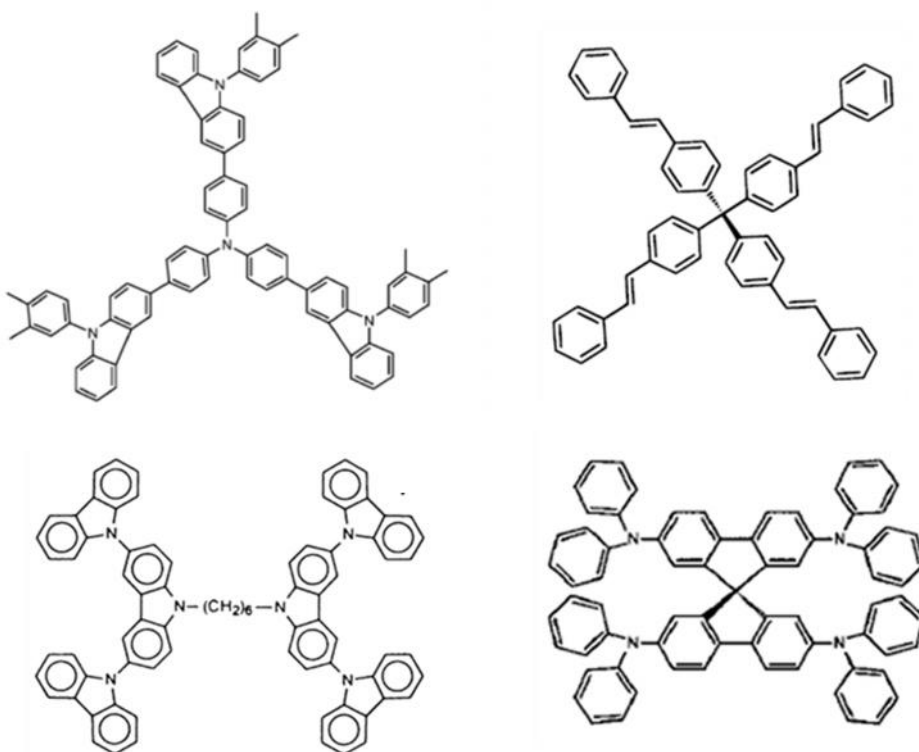


Figure 1.7. Examples of molecular resists⁵⁸⁻⁶⁴

There are several reasons why scientists are interested in molecular glass resists. Molecular glasses can be monodisperse (size $\sim 1 - 2$ nm) with well- defined molecular structures. Classical polymeric resists have wide molecular weight distribution compared to molecular glasses due to chain entanglement⁶⁵. Molecular glasses can have characteristic properties of small molecules, like high purity and well defined structures. They can also

have beneficial aspects of polymers, such as high thermal stability and thin film forming properties⁴⁸. In Figure 1.8, size comparison of a typical polymer resist and a molecular glass resist is shown.

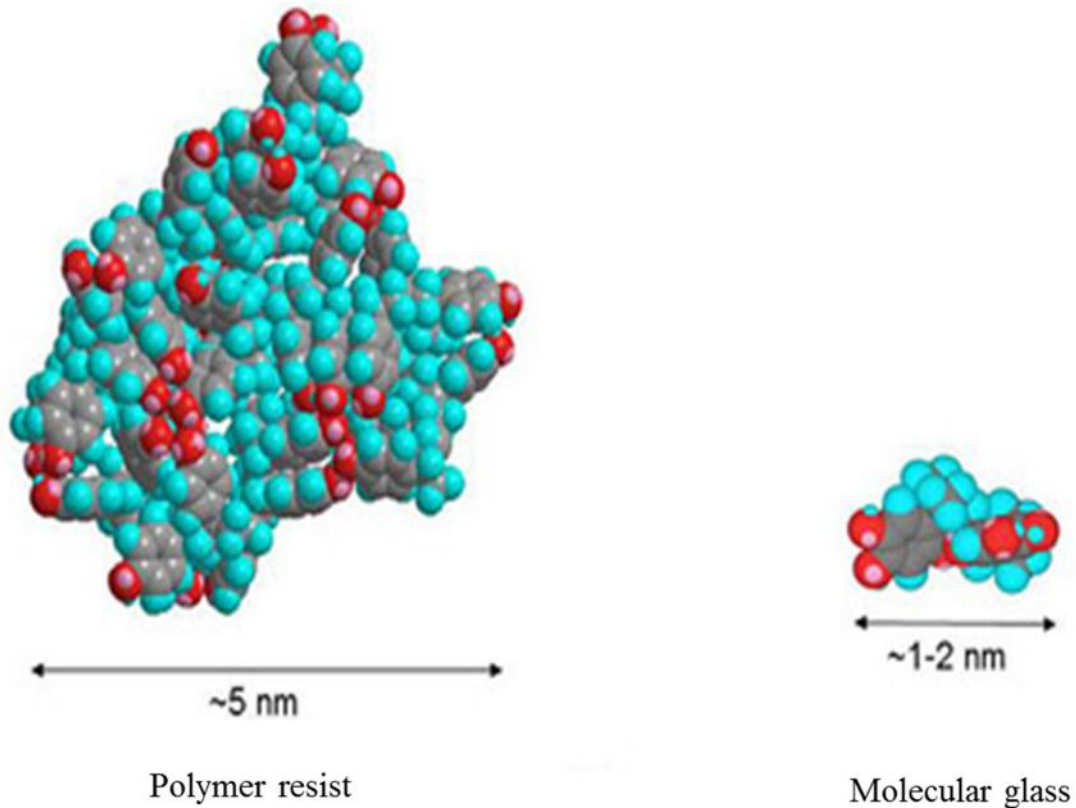


Figure 1.8. Size comparison between a typical polymer resist and a typical molecular glass⁵⁶

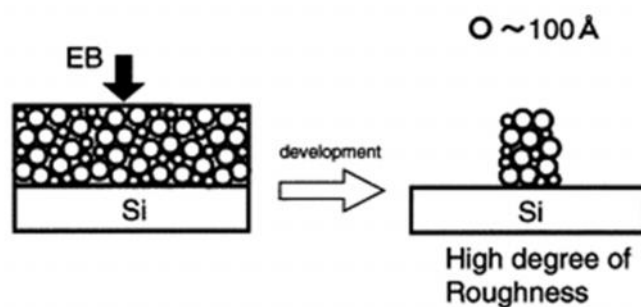
Utilizing molecular glass resists is believed to be a fundamental improvement in the ability to consistently obtain high resolution patterns. Size compatibility of molecular glass resist and resist additives (like photoacid generator), results in having a uniform phase. Molecular glass resists are also free of intermolecular chain entanglement, which enhances their uniformity. Furthermore, molecular glass resists are likely to make

significant contributions to minimize line edge roughness (LER) in very small feature sizes^{51,66}.

It has been reported by Shirota and coworkers that the free volume in MGs is distributed into much smaller units compared to polymeric materials^{54,67}. In addition to having smaller sized MG, the distribution of free volume in MG systems can affect patterning performance. The MG resist building block may be as much as an order of magnitude smaller than conventional polymeric resists. Reduction of the “pixel” size is a fundamental improvement in the ability to obtain high resolution patterns. Figure 1.9 shows volume comparison between polymer and molecular glass resist and its effect in increasing resolution in photolithography.

Theoretical studies have shown that LER decreases with reduced molecular weight of the photoresist, both for classical and chemically amplified photoresists. It can be hypothesized that size and distribution of free volume may also affect diffusion kinetics in the MG resist matrix⁵¹.

Polymer Resist Materials



Molecular Resist

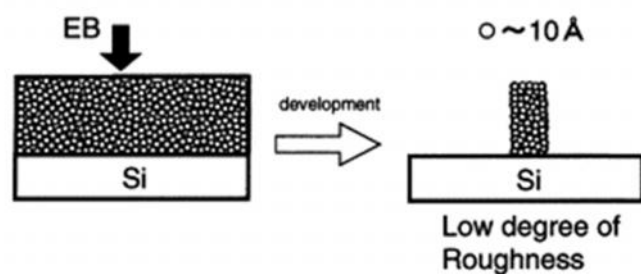


Figure 1.9. Volume comparisons between polymer resist and molecular glass⁵⁴

Diffusion of generated acid from resist additives can have adverse effects on patterning, such as limiting the resolution and causing pattern fluctuations⁶⁶. Hence, inherent molecular features that can limit acid diffusion should be considered in designing MG resist, since it helps in achieving higher resolution features and lower LER.

Another important factor that needs to be considered in designing a MG resist is its glass transition temperature (T_g). Having high T_g shows the ability to form stable thin films. Molecular glass resists often show high thermal stability and high glass transition temperatures (T_g)^{55,67}. Photoresists undergo several steps such as post exposure bake

(PEB), base development, and etching in lithography. For successful processing in PEB, the resist material should be heated below its T_g . Post exposure bake (PEB) step is an essential step in the process of making resist pattern. For positive tone resists, the thermal energy is provided for enabling acid catalyzed reaction. For negative tone resists, the required energy for crosslinking is provided in this step. If the PEB step is carried out at a temperature above the T_g of photoresist material, it can cause contrary effects such as limiting resolution, and making distortion in the pattern. Heating above T_g of the photoresist can also accelerate acid diffusion during PEB step, which can increase LER⁴⁸.

In conclusion, due to molecular glasses promising properties, they have been considered as alternative choice to polymeric resists for the next generation of photoresists.

1.6 Molecular Design

The molecular architecture is important for creating a dense, bulky, high T_g molecular resist system. Several approaches in designing stable MGs have been discussed in literature^{48,68}. Since the aim is to design amorphous molecular materials, two criteria should be considered based on structural features: high T_g , and low crystal growth rate. One relevant structural feature is asymmetry. In asymmetric structures, molecules tend to have glass formation and low crystal growth rate, due to difficulties in molecular packing. On the other hand, T_g may decrease, because there are more free volume in asymmetric structures. Hence, a careful attention is required when considering structural features and different moieties in designing a molecular glass resist. Structural features for increasing T_g , that decrease free volume and restrict rotation around molecular axis have been

studied. This includes having rigid and bulky groups such as biphenyl, and fluorene moieties in the structure. These moieties can raise T_g by hindering translational, rotational, and vibrational modes of the molecule⁶⁹. Furthermore, the presence of intermolecular interactions, such as dipole–dipole and hydrogen bonding interactions increase T_g by decreasing the free volume. These fundamental concepts have been applied in synthesizing several thermally stable inorganic and organic systems with high T_g⁴⁸.

In this thesis, preliminary results on several negative and positive tone molecular glass resists are presented. Three main cross-linking functional groups (acrylate, oxetane, and epoxy) are explored in synthesizing molecular glass resists. These compounds are synthesized or purchased as model materials for the study of thermal network cross-linking and are examined for solubility in developer solvents.

1.7 References

- (1) Sugihara, M. In *Recent Advances in Nanofabrication Techniques and Applications*; Cui, B., Ed.; InTech: **2011**, p 69.
- (2) Moore, G. *Electronics Magazine* **1965**, 38.
- (3) Moore, G. *Proceedings of SPIE* **1995**, 2437, 2.
- (4) http://edu.cs.tut.fi/SA2007/EPs_intro.html 2013.
- (5) Borodovsky, Y. **2006**, 6153.
- (6) <http://www.lithoguru.com/scientist/lithobasics.htm>.
- (7) Yeh, W.-M.; Noga, D. E.; Lawson, R. A.; Tolbert, L. M.; Henderson, C. L. *Journal of Vacuum Science & Technology B: Microelectronics and Nanometer Structures* **2010**, 28, C6S6.
- (8) Martin, C.; Rius, G.; Llobera, A.; Voigt, A.; Gruetzner, G.; F.Perez-Murano *Microelectronic Engineering* **2007**, 84, 1096.
- (9) Beuret, C.; Racine, G.-A.; Gobet, J.; Luthier, R.; Rooij, N. F. d. *MEMS '94 Proceedings, IEEE Workshop* **1994**, 81.
- (10) Yoon, Y.-K.; Park, J.-H.; Allen, M. G. *Journal of Microelectromechanical Systems* **2006**, 15, 1121.
- (11) Montelius, L.; B. Heidari; Graczyk, M.; Maximov, I.; Sarwe, E.-L.; Ling, T. G. I. *Microelectronic Engineering* **2000**, 53, 521.
- (12) Bertsch, A.; Lorenz, H.; Renaud, P. *Sensors and Actuators A: Physical* **1999**, 73, 14.
- (13) Lin, B. J. *Journal of Vacuum Science and Technology* **1975**, 12, 1317.
- (14) Kawamura, Y.; Toyoda, K.; Namba, S. *Journal of Applied Physics* **1982**, 53, 6489.
- (15) Iwayanagi, T.; Kohashi, T. A.; Nonogaki, S.; Matsuzawa, T.; Douta, K.; Yanazawa, H. *IEEE Transactions on Electron Device* **1981**, 28, 1306.
- (16) Fontana, R. E.; Katine, J.; Rooks, M.; Viswanathan, R.; Lille, J.; MacDonald, S.; Kratschmer, E.; Tsang, C.; Nguyen, S.; Robertson, N.; Kasiraj, P. *IEEE TRANSACTIONS ON MAGNETICS* **2002**, 38.

- (17) Liu, K.; Avouris, P.; Bucchignano, J.; Martel, R.; Sun, S.; Michl, J. *Applied Physics Letters* **2002**, *80*, 865.
- (18) Marrian, C. R. K. *Journal of Vacuum Science & Technology B: Microelectronics and Nanometer Structures* **1992**, *10*, 2877.
- (19) Wu, B.; Kumar, A. *Journal of Vacuum Science & Technology B: Microelectronics and Nanometer Structures* **2007**, *25*, 1743.
- (20) Gwyn, C. W. *Journal of Vacuum Science & Technology B: Microelectronics and Nanometer Structures* **1998**, *16*, 3142.
- (21) Gullikson, E. M.; Cerjan, C.; Stearns, D. G.; Mirkarimi, P. B.; Sweeney, D. W. *Journal of Vacuum Science & Technology B: Microelectronics and Nanometer Structures* **2002**, *20*, 81.
- (22) McCord, M. A.; Rooks, M. J. *Handbook of Microlithography, Micromachining, and Microfabrication, SPIE*; P. R. Choudhury ed., **1997**, 1
- (23) Cheng, J. Y.; Ross, C. A.; Smith, H. I.; Thomas, E. L. *Advanced Materials* **2006**, *18*, 2505.
- (24) May, G. S.; Sze, S. M. *Fundamentals of Semiconductor Fabrication*; John Wiley and Sons, Inc., **2004**.
- (25) Lawson, R. A., Georgia Institute of Technology, **2011**.
- (26) Dai, J.; Chang, S. W.; Hamad, A.; Da Yang, N. F.; Ober, C. K. *Chem. Mater.* **2006**, *18*, 3404.
- (27) Nakayama, T.; Ueda, M. *J. Mater. Chem.* **1999**, *9*, 697.
- (28) Tully, D. C.; Wilder, K.; Fre'chet, J. M. J.; Trimble, A. R.; Quate, C. *Adv. Mater.* **1999**, *11*, 314.
- (29) Yoshiiwa, M.; Kageyama, H.; Shirota, Y.; Wakaya, F.; Gamo, K.; Takai, M. *Appl. Phys. Lett.* **1996**, *69*, 2605.
- (30) Reichmanis, E.; Houlihan, F. M.; Nalamasu, O.; Neenan, T. X. *Chem. Mater.* **1991**, *3*, 394.
- (31) Willson, C. G.; Trinque, B. C. *J. Photopolym. Sci. Technol.* **2003**, *16*, 621.
- (32) Ito, H. *J. Photopolym. Sci. Technol.* **1998**, *11*, 379.
- (33) Lin, Q.; Sooriyakumaran, R.; Huang, W. *Proc. SPIE* **2000**, *3999*, 230.

- (34) Shin, J.; Ma, Y.; Cerrina, F. *J. Vac. Sci. Technol., B.* **2002**, *20*, 2927.
- (35) Rau, N.; Stratton, F.; Fields, C.; Ogawa, T.; Neureuther, A.; Willson, G. *J. Vac. Sci. Technol., B.* **1998**, *16*, 3784.
- (36) Asakawa, K.; Ushirogouchi, T.; Nakase, M. *J. Vac. Sci. Technol., B.* **1995**, *13*, 833.
- (37) Shiraishi, H.; Yoshimura, T.; Sakamizu, T.; Ueno, T.; Okazaki, S. *J. Vac. Sci. Technol., B.* **1994**, *12*, 3895.
- (38) He, D.; Cerrina, F. *J. Vac. Sci. Technol., B.* **1998**, *16*, 3748.
- (39) Ban, Y.; Sundareswaran, S.; Pan, D. Z. *J. Micro/Nanolith. MEMS MOEMS*, **2010**, 041206.
- (40) <http://ece.iisc.ernet.in/~kjvinoy/rfmems/set2.pdf>.
- (41) Dammel, R. R. *J. Microlith., Microfab., Microsyst.* **2002**, *1*, 270.
- (42) <https://sites.google.com/site/hendersonresearchgroup/helpful-primers-introductions/helpful-primers>.
- (43) Anguang Yu; Heping Liu; James P. Blinco; Kevin S. Jack; Michael Leeson; Todd R. Younkin; Andrew K. Whittaker; Blakey, I. *Macromol. Rapid Commun.* **2010**, *31*, 1449.
- (44) http://researcher.watson.ibm.com/researcher/view_project_subpage.php?id=3662.
- (45) http://www.future-fab.com/documents.asp?d_ID=2614.
- (46) Henderson, C. L.; Nishimura, I.; Heath, W. H.; Matsumoto, K.; Jen, W.-L.; Lee, S. S.; Neikirk, C.; Shimokawa, T.; Ito, K.; Fujiwara, K.; Willson, C. G. **2008**, *6923*, 69231C.
- (47) Dammel, R. R. *SPIE Optical Engineering Press* **1993**.
- (48) Anuja De Silva; Jin-Kyun Lee; André, X.; Felix, N. M.; Cao, H. B.; Deng, H.; Ober, C. K. *Chem. Mater.* **2008**, *20*, 1606.
- (49) Cao, H.; Yueh, W.; Rice, B.; Roberts, J.; Bacuita, T.; Chandhok, M. *Adv. Resist Technol. Process. XXI* **2004**, *5376*, 757.
- (50) Fedynyshyn, T. H.; Pottebaum, I.; Astolfi, D. K.; Cabral, A.; Roberts, J.; Meagley, A. R. *J. Vac. Sci. Technol., B* **2006**, *24*, 3031.

- (51) Kadota, T.; Kageyama, H.; Wakaya, F.; Gamo, K.; Shirota, Y. *Materials Science and Engineering C*. **2001**, *16*, 91.
- (52) J. Fujita; Y. Ohnishi *App. Phys. Lett.*, **1996**, *68*, 1297.
- (53) Montague, M. F.; Hawker, C. J. *Chem. Mater.* **2007**, *19*, 526.
- (54) Strohriegl, P.; Grazulevicius, J. V. *Advanced Materials* **2002**, *14*, 1439.
- (55) Plante, A.; Palato, S.; Lebel, O.; Soldera, A. *Journal of Materials Chemistry C* **2013**, *1*, 1037.
- (56) Yang, D.; Chang, S. W.; Ober, C. K. *Journal of Materials Chemistry* **2006**, *16*, 1693.
- (57) Patsis, G. P.; Constantoudis, V.; Gogolides, E. *Microelectronic Engineering* **2004**, *75*, 297.
- (58) Bettenhausen, J.; Strohriegl, P. *Adv. Mater.* **1996**, *8*, 507.
- (59) Sonntag, M.; Kreger, K.; Hanft, D.; Strohriegl, P. *Chem. Mater.* **2005**, *17*, 3031.
- (60) Grigalevicius, S.; Blazys, G.; Ostrauskaite, J.; Grazulevicius, J. V.; Gaidelis, V.; Jankauskas, V. *J. Photochem. Photobiol., A*. **2003**, *154*, 161.
- (61) Theissen, U.; Zilker, S. J.; Pfeuffer, T.; Strohriegl, P. *Adv. Mater.* **2000**, *12*, 1698.
- (62) Wang, S. J.; Raymond, A.; Hudack, J.; Bazan, G. C. *J. Am. Chem. Soc.* **2000**, *122*, 5695.
- (63) Reichert, V. R.; Mathias, L. J. *Macromolecules* **1994**, *27*, 7015.
- (64) Steuber, B. F.; Staudigel, J.; Stössel, M.; Simmerer, J.; Winnacker, A.; Spreitzer, H.; Weissörtel, F.; Salbeck, J. *Adv. Mater.* **2000**, *12*, 130.
- (65) Henderson, C. L.; De Silva, A.; Felix, N.; Sha, J.; Lee, J.-K.; Ober, C. K. **2008**, 6923, 69231L.
- (66) De Silva, A.; Felix, N. M.; Ober, C. K. *Advanced Materials* **2008**, *20*, 3355.
- (67) Shirota, Y. *J. Mater. Chem.* **2005**, *15*, 75.
- (68) Shizuo, T.; Hiromitsu, T.; Koji, N.; Akane, O.; Yasunori, T. *Appl. Phys. Lett.* **1997**, *70*, 1929.
- (69) Liu, X.-M.; He, C.; Huang, J.; Xu, J. *Chem. Mater.* **2005**, 434.

CHAPTER 2 -ACRYLATE-BASED RESISTS AND STUDYING PATTERNING PERFORMANCE

2.1 Introduction

Acrylates have many applications in industry including coatings, adhesives, dental restorative materials, information storage systems, and lithographic materials¹⁻³. Multifunctional (meth)acrylate resins have been widely used as photosensitive materials in printing plates, inks, photoresists, coatings and photo-curable adhesives⁴. These compounds are one of the materials used in both positive and negative tone resists in lithography. Also, acrylate monomers are the most widely studied for step and flash lithography⁵⁻⁸. Acrylates have been known as photo-polymerizable materials due to their ability to make highly cross-linked networks. This feature gives them many desirable properties such as high strength, low moisture adsorption, and rapid curing. Acrylate compounds are usually polymerized by a free radical polymerization method that utilizes their unsaturated bonds in the polymerization. This method is the most common nonliving polymerization method⁹. In a free radical polymerization process, the first step starts with initiation, where an initiator decomposes into radicals under reaction conditions such as heat or radiation. The next step is the propagation step, where the primary radical produced in initiation step attacks a carbon double bond of the monomer, and makes a new radical species which continues the chain. The last step is a termination step, where several different mechanisms can intervene, such as coupling or disproportionation.

has other desirable properties mentioned above. These great properties and high cross linking make acrylate a good choice for studying in negative tone photoresist.

2.2 Thermal Curing Procedure

In order to test the extent of cross-linking, a multi-functional acrylate compound was mixed with azobisisobutyronitrile (AIBN), a thermal radical initiator. Films were coated on Silicon wafer and heated to initiate cross-linking. The extent of cross-linking at different temperatures was studied by washing the cross-linked film with solvent, and measuring the normalized remaining thickness (NRT) relative to the unwashed thermally cross-linked film.

A solution of 3-10 wt% acrylate in propylene glycol monomethyl ether acetate (PGMEA) with 10 mol% AIBN relative to acrylate compound was made and spin coated at 1000-2000 rpm on a Silicon wafer. The film was baked at 30-180°C for 10 minutes under N₂ purge. The film was cut in two pieces. One piece was kept as the unwashed reference sample for later comparison. The other piece was washed with solvent developers such as methyl isobutyl ketone (MIBK), or MeOH, by immersing the piece for 2 minutes. The film was rinsed with isopropyl alcohol (IPA), and dried with N₂ purge. The solvent developers wash away the lower molecular weight fragments. MIBK and MeOH are highly compatible with a variety of organic reagents and are good solvents for a wide range of industrial materials. Figure 2.2 shows the chemical structure of solvents used in thermal curing procedure.

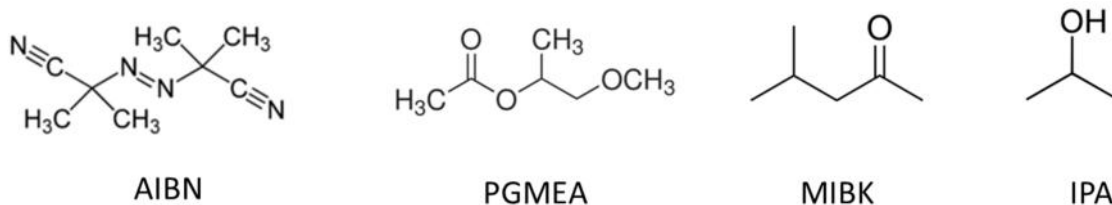


Figure 2.2. Chemical Structure of solvents used in thermal curing procedure

The film thicknesses for the unwashed and washed samples were measured with spectroscopic ellipsometry, using a Cauchy layer with a silicon underlayer and 1.5 nm silicon oxide.

2.3 Materials and Instruments

Unless otherwise noted, all reagents and solvents were purchased from Sigma-Aldrich, TCI America, or Alfa-Aesar and were used as received. A Varian Mercury Vx 300 instrument was used to measure NMR spectra.

2.4 BHPF (9,9-bis(4-hydroxyphenyl)fluorene)

BHPF (9,9-bis(4-hydroxyphenyl)fluorene) has multiple aromatic rings in the molecule. Due to geometric constraints, the fluorene unit and the aryl groups cannot be in the same plane. In these types of compounds, each aromatic ring occupies a different plane¹³. (See Figure 2.3)

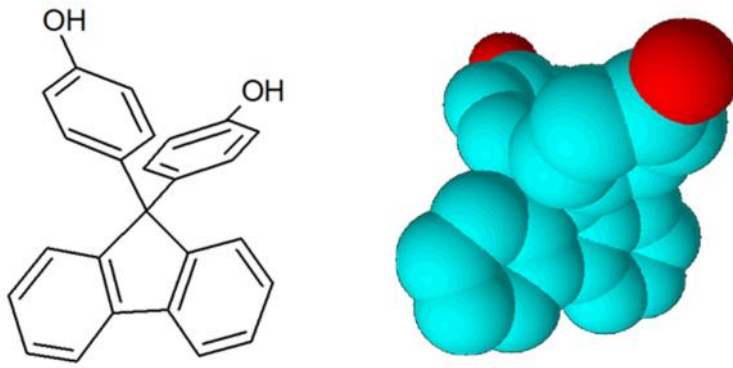


Figure 2.3. Structures of 9,9-bis(4-hydroxyphenyl)fluorene (BHPF)

BHPF is a “cardo” structure, and has been reported in the literature¹³. A cardo polymer is part of a series of high Tg polymers. This series of polymer was prepared in the early 1960s and was studied by Korshak *et al.*^{14,15}. The polymer structure is based on the position of fluorene similar to wings and body of a butterfly, which is the origin of the name¹⁶. In these compounds, a cyclic side group, with structure-based diol components as a backbone, lead to increased thermal stability, high Tg, and improved solubility of polymer in organic solvents¹⁴. Hsiao *et al.* showed that incorporation of the ether functionality and a fluorene group into the polymer backbone, results in aromatic polyamides, polyimides, and poly(amide-imide)s with good thermal stability and high Tg^{14,17-19}. Recently, synthesis of aromatic polyazomethines was reported by reaction of diphenylfluorene with dialdehyde moiety and aromatic diamines. This polymer has a good organic solubility, high Tg, and reasonable thermal stability²⁰.

BHPF was selected in this work as the starting molecule of polymer backbone. The acrylate group was selected for polymerization, because of its high cross-linking property that results in stable polymer with high Tg. In this work, BHPF was functionalized with methacrylate group for negative tone photoresist application.

2.4.1 Synthesis of BHPF-2MA

Figure 2.4 shows the reaction for functionalizing 9,9-bis(4-hydroxyphenyl)fluorene (BHPF) with the methacrylate group. A 3.5 g portion (0.01 mole, 1 eq) of (BHPF) and 2.02 g (0.02 mole, 2 eq) of triethylamine was dissolved in 10 mL of dry ether. Then, 2.2 g (0.02 mole, 2 Eq) of methacryloyl chloride was added dropwise to the solution under cooling with ice water. The reaction was continued at room temperature for 1.5 hrs. A white precipitate (triethylammonium chloride) was separated by filtration, and the ether was evaporated under reduced pressure from the filtrate. The resulting solid was purified by flash chromatography using dichloromethane, to yield 50% (2.4g) white powder.

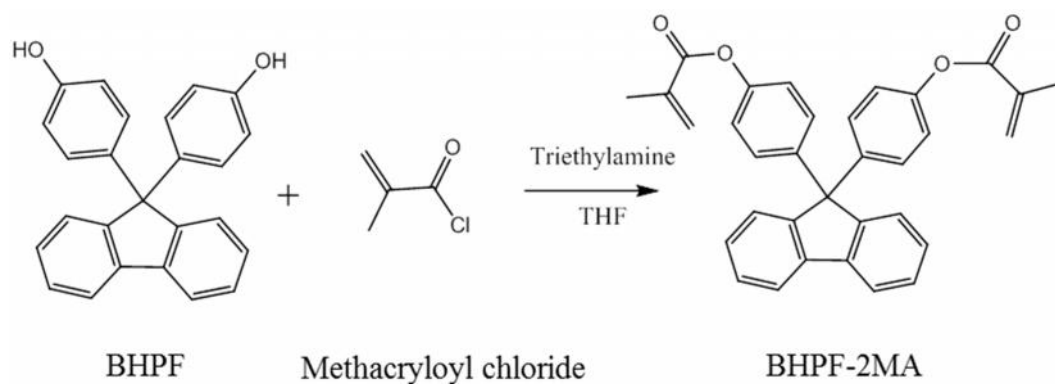


Figure 2.4. Synthesis of BHPF-2MA

After synthesis, the structure was confirmed by $^1\text{H-NMR}$. NMR (300 MHz, DMSO- d_6) δ (ppm), 1.96 (s, 6H), 5.87 (m, 2H), 6.23 (m, 2H), 7.12 (m, 8H), 7.39 (m, 6H), 7.96 (m, 2H). IR (KBr): 3010-3150 (= CH stretch), 2800-2950 (aliphatic C-H stretch), 3000-3020 (aromatic C-H stretch) 1741 (C=O stretch of ester), 1637 (C=C stretch), 1465 (CH_2 bend) 1379 (CH_3 bend) 1140-1215 (C-O-C).

After successfully synthesizing BHPF-2MA, thermal curing was performed on it to assess its suitability as a negative tone photoresist.

2.4.2 Thermal Curing of BHPF-2MA

Thermal curing for BHPF-2MA was performed at different temperatures, and for each temperature, the measured film thickness of the washed sample was normalized to the unwashed film thickness at the same temperature.

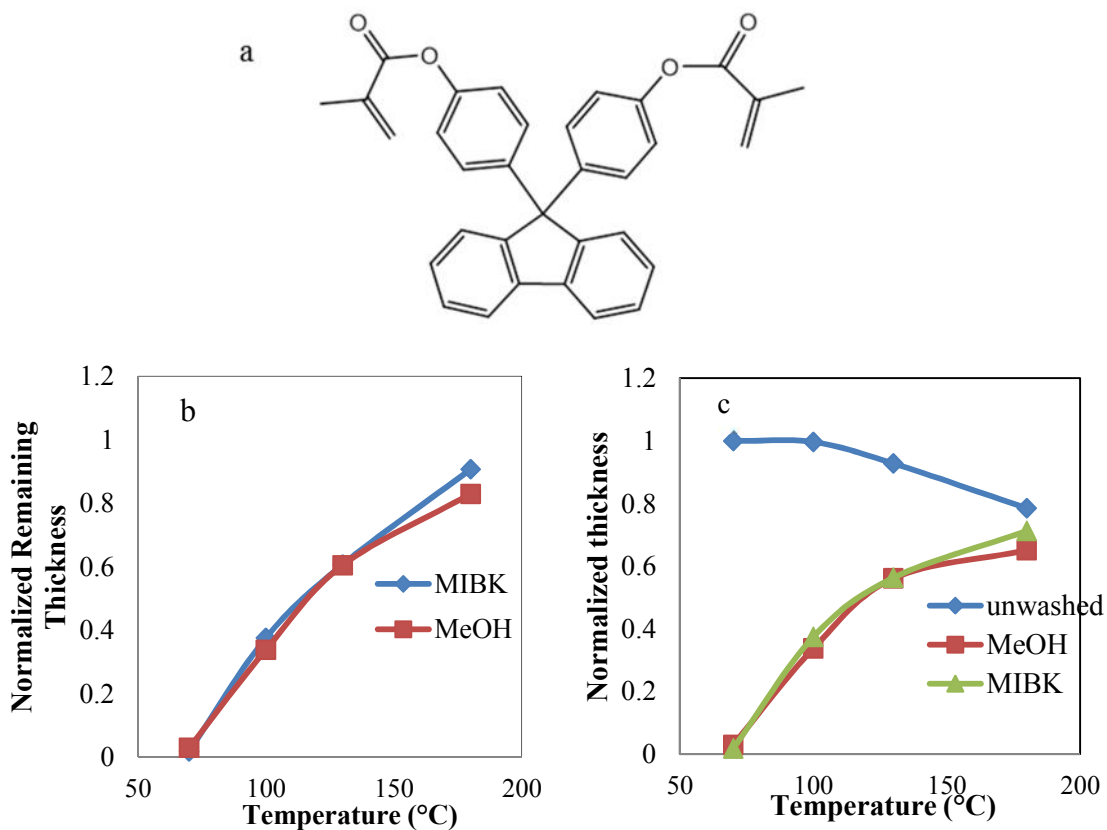


Figure 2.5. Structure of BHPF-2MA (a), NRT as a function of temperature in MIBK or MeOH (b). Normalized thickness to unwashed thickness of 70°C (c)

As shown in Figure 2.5 (b), normalized remaining thickness (NRT) increases with increasing temperature. In Figure 2.5 (c), slight thickness loss was seen in the unwashed

film at 130°C. Also, it can be seen on Figure 2.5 (a) that NRT is closed to 1 at 180°C. However, the unwashed sample at 180°C shows significant loss of thickness compared to its thickness at 70°C. This loss of thickness is likely due to expected shrinkage of acrylate during crosslinking. The shrinkage is most likely due to the replacement of weak and long distance intermolecular van der Waals bonds, by stronger and shorter covalent bonds between the carbon atoms of different monomer units during polymerization. Shrinkage in polymerization process is a common phenomenon and a major cause for materials failures and shortened service life²¹. This is also one of the concerns for curing acrylates and affects the adhesion to the substrate²²⁻²⁵.

In short, BHPF-2MA does not give a desired NRT of 1 while keeping the unwashed thickness constant. One of the ways for solving the shrinkage problem is to use flexible monomers. This can reduce the volume shrinkage during polymerization²².

2.5 Thermal Curing of Trimethylolpropane Triacrylate (TMPTA)

Since BHPF-2MA (with two cross-link groups) only goes to NRT of 0.6 in thermally stable crosslink temperatures, having a molecule with more cross-link groups on a flexible aliphatic core might improve the likelihood of reaching the desired NRT of 1.0. Typically, compounds with highly functional acrylate monomers are used for rapid polymerization. Furthermore, these highly cross-linked networks cause less shrinkage compared to networks formed from monomers with lower functionality²².

Trimethylolpropane triacrylate (TMPTA) is a trifunctional monomer that is mostly used in manufacturing plastic, adhesive, acrylic glue, anaerobic sealant, and Ink²⁶. TMPTA has three acrylate groups that can be used to enhance cross linking of

photopolymerization^{27,28}. TMPTA is commercially available as a cross-linking additive and can be used in coatings, compact discs, hardwood floors, dental polymers, lithography, screen printing, elastomers, and medical industry.

The cross-linking of TMPTA was tested using a procedure similar to that listed for BHPF-2MA, except that the TMPTA (as purchased and received) was passed through an alumina column to remove any inhibitor before making the resist solution.

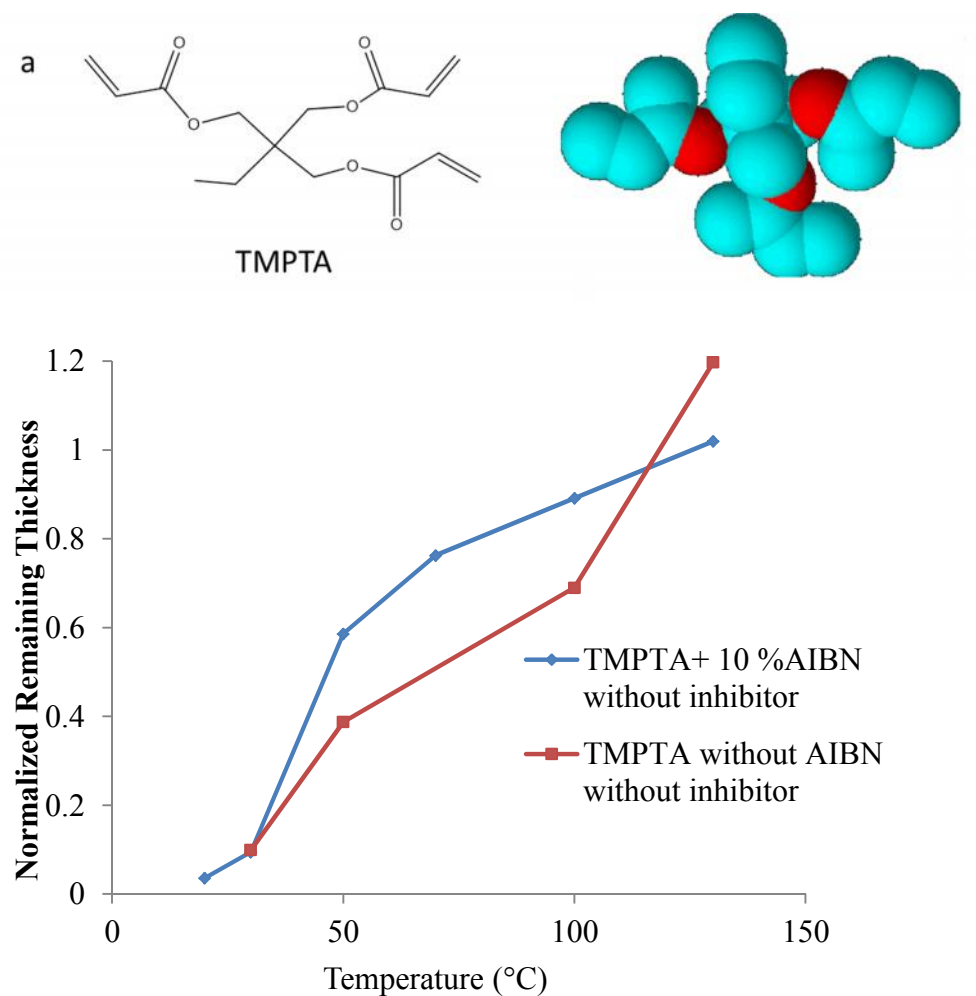


Figure 2.6. TMPTA structure (a), and NRT as a function of temperature (b)

In the curing procedure, 10 mol% AIBN was added to some solutions before spin coating. TMPTA was spin coated with and without 10 mol% AIBN. Figure 2.6 shows the

structure of TMPTA, and NRT of TMPTA, with and without 10 mol% AIBN. As shown in Figure 2.6, TMPTA with 10 mol% AIBN showed poor cross-linking below 50°C. This is due to known inadequate decomposition of AIBN below 65°C. TMPTA with 10 mol% AIBN successfully reached NRT of 1 at 130°C with no apparent decomposition. The observation of NRT higher than 1 (at 130°C) for TMPTA without AIBN is likely due to swelling during development.

In order to further study the TMPTA polymerization and crosslinking, no AIBN (radical initiator) was added to TMPTA in the next experiment. In Figure 2.6, significant auto thermal polymerization was observed for TMPTA films. Due to TMPTA polymerization, even without a radical initiator, this compound is not suitable for photoresist applications. This is because almost no contrast would exist between UV exposed and unexposed regions of TMPTA film

2.6 Relationship between Structure and Property

In order to avoid autopolymerization, we chose less functionalized acrylate compounds for the next experiments, anticipating that the kinetic chain length would decrease with the enhanced bulkiness of the middle part of the monomers. The reason for this might be due to low mobility of the monomers which causes a short kinetic chain length²⁹. Bisphenol A was chosen as the backbone for studying thermal curing properties.

Three commercially available diacrylates: bisphenol A dimethacrylate (BPA-2MA), bisphenol A glycerolate dimethacrylate (BPA-G-2MA), and bisphenol F ethoxylate (2 EOphenol) diacrylate (BPF-2A) were selected. Figure 2.7 shows the chemical structure of these compounds. BPA-G-2MA has a much more flexible

connecting structure than BPA-2MA. BPA-2MA crystallizes upon spin-coating, due to its relatively rigid structure. The other two compounds form sufficiently stable amorphous films due to their flexible arms that inhibit crystallization.

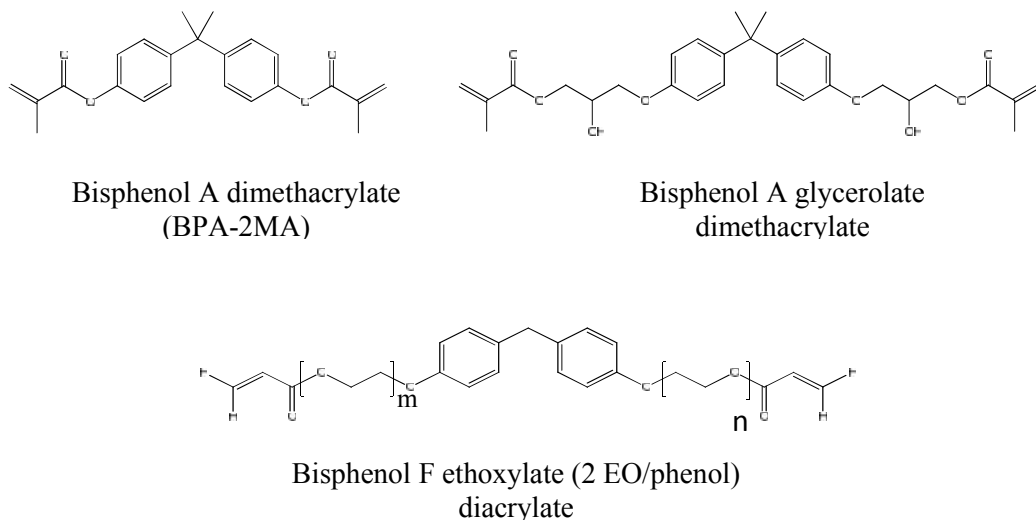


Figure 2.7. Chemical structure of BPA-2MA, BPA-G-2MA, and BPF-2A

2.7 Thermal Curing of BPF-2A

Bisphenol F ethoxylate (2 EO/phenol) diacrylate (BPF-2A) is a difunctional acrylate monomer, whose structure is shown in Fig. 2.7. It can be readily polymerized by UV-curing. This compound is selected due to highly cross-linked, and, resistant up to 300°C³⁰⁻³². This compound was passed through alumina column to remove inhibitor (100 ppm monomethyl ether hydroquinone). Cross-linking of this compound was tested using similar thermal curing procedure explained earlier, after the inhibitor was removed. In Figure 2.8, the structure of BPF-2A and its NRT at different temperatures are shown. Similar to BHPF-2MA, this compound could not efficiently cross-link to sufficiently insolubilize the film (max NRT ~ 0.6).

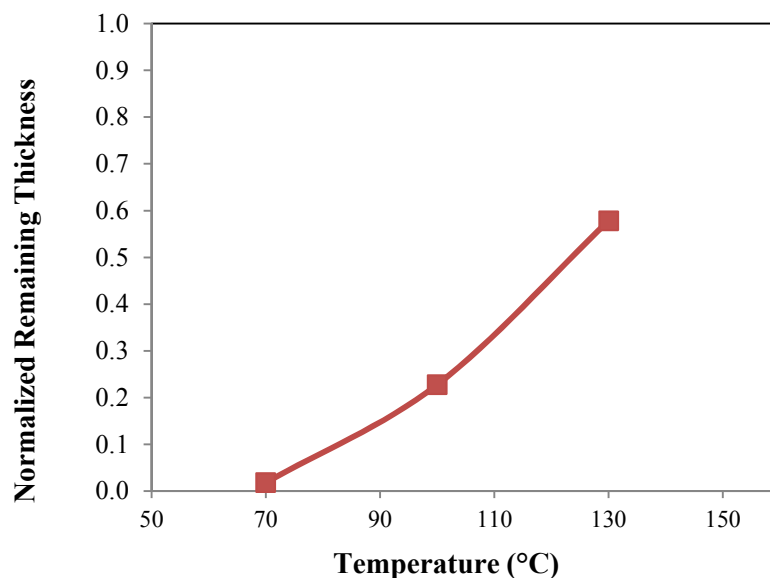


Figure 2.8. BPF-2A structure and NRT as a function of temperature for BPF-2A film

2.8 Thermal Curing of BPA-G-2MA

Bisphenol A glycerolate dimethacrylate (BPA-G-2MA) is a cross-linking compound with two functional groups. This compound was purchased and thermally cured according to the procedure mentioned earlier (see above). In Figure 2.9, the structure of BPA-G-2MA and its NRT at different temperatures are shown. Similar to BPF-2A, this compound could not efficiently cross-link to sufficiently insolubilize the film. BPA-G-2MA showed slightly better performance than previous polyphenolic compounds, but still did not reach sufficient NRT for photoresist applications.

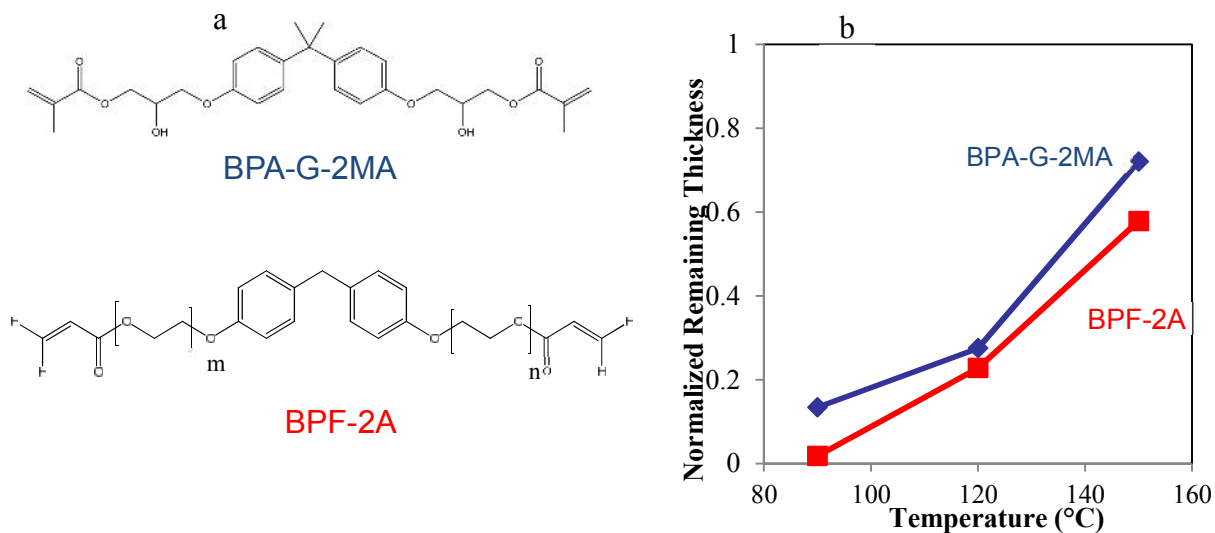


Figure 2.9. Structures of BPA-G-2MA and BPF-2A (a), and NRT as a function of temperature for BPA-G-2MA, and BPF-2A films (b)

Difunctional polyphenolic molecular resists using acrylate (BPF-2A) and methacrylate (BPA-G-2MA) cross-linking groups have shown apparent issues in reaching the desired NRT.

2.9 Auto Thermal Polymerization Characterization

For further characterization, these compounds need to be checked for the absence of auto-thermal polymerization, as this would be the limiting factor in using them as photoresist materials. Auto-thermal polymerization of BPA-G-2MA was studied. For this experiment, BPA-G-2MA solution was spin coated on Silicon wafer with no initiator (AIBN) and was baked at 130°C for different durations. As it is seen in Figure 2.10, auto-thermal polymerization was seen for this compound, which is a significant problem. The extent of the reaction increased with time. These kinds of acrylate compounds with the studied backbone showed problems such as shrinkage and auto-thermal polymerization and thus were not suitable as negative tone resist material.

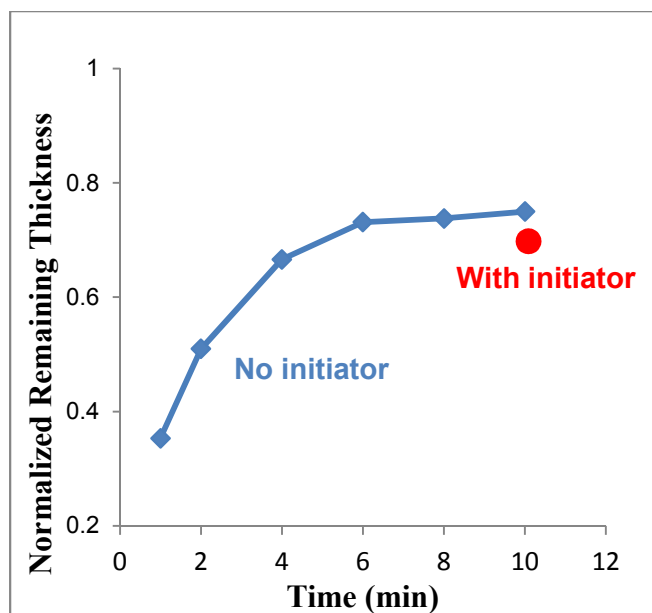


Figure 2.10. NRT as a function of temperature for BPA-G-2MA, with and without initiator (AIBN) at 130°C

2.10 Positive tone Cross-Linking

Another part of this research is to design and synthesize positive tone photo resists for to their enhanced adhesion and mechanical strength compared to negative tone resists. Positive tone resists have reduced swelling compared to polymeric cross-linked negative tone resists. They also have increased mobility of photoacid in the middle of exposed regions, but not at line edges which results in increasing sensitivity and reducing blur. Recently, some positive tone photoresist which are thermally or chemically degradable under appropriate condition have been reported³³⁻³⁶. The concept of disconnecting thermoset networks was described for epoxy systems that form networks with disulfide linkages³⁷. Cycloaliphatic diepoxides with cleavable acetal links have also been studied, which provide networks that are easily decomposed in acidic condition³⁸.

Ober *et. al* reported the incorporation of tertiary esters in epoxy compounds and demonstrated their potential uses as photoresist materials³⁹.

Based on the literature review for positive tone resists, in our molecular design, acrylate was used for cross-linking, and a tertiary ester was used as an acid cleavable group. A tertiary ester is subject to breakdown into carboxylic acid and alkene during post exposure bake. Figure 2.11 shows the process for developing a positive tone photoresist.

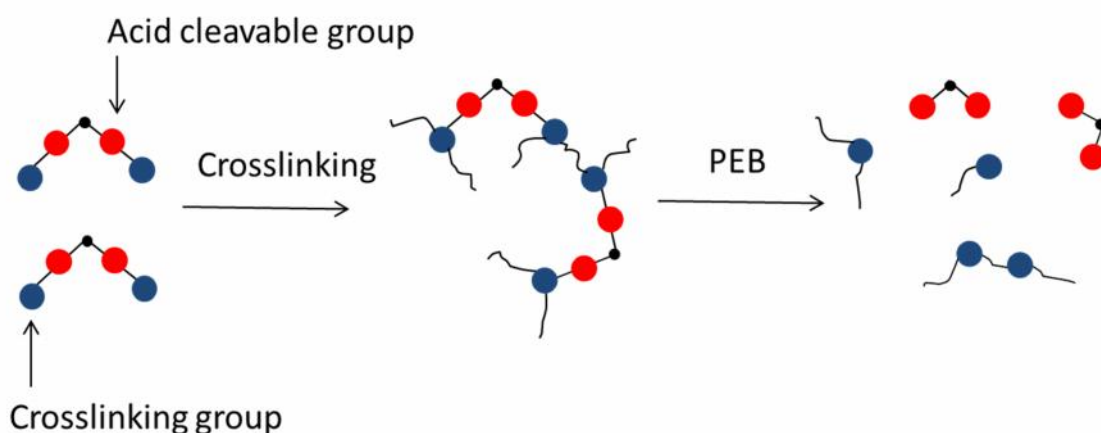


Figure 2.11. Process for developing positive tone photoresist

2.10.1 Synthesis of Hex-2MA

Hex-2MA has been synthesized and studied for its cross-linking properties. Hex-2MA was designed to allow investigation of both positive tone cross-linking systems. As shown in Figure 2.12, Hex-2MA was thermally cross-linked and because the tertiary ester bond is weak, could be decomposed by a photoacid generator.

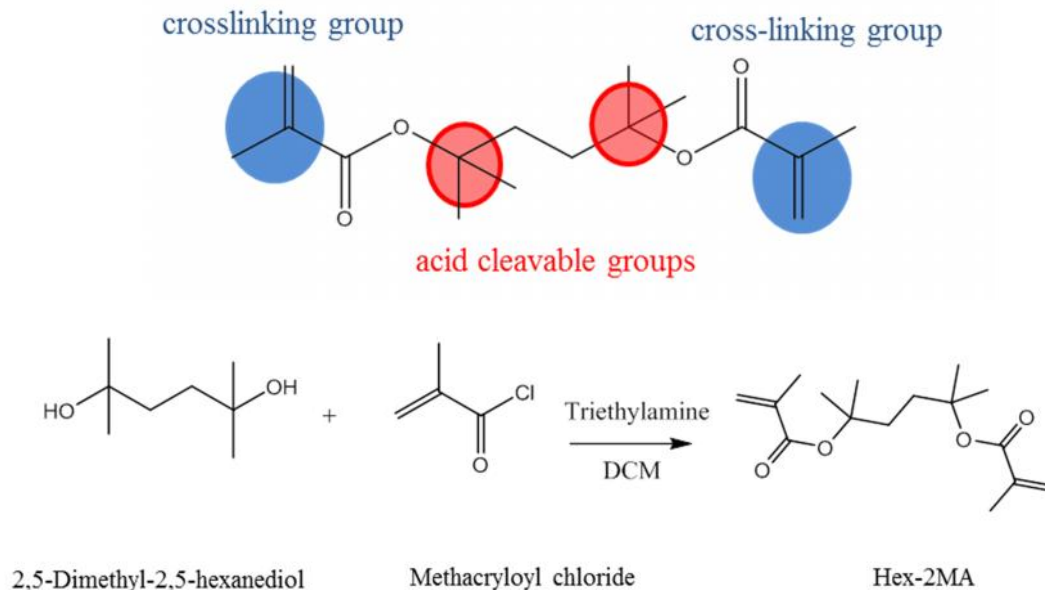


Figure 2.12. Structure of Hex-2MA (a), and synthesis reaction for Hex-2MA (b)

The following is the procedure for synthesis of Hex-2MA: 3.65g (0.025 mole, 1 eq) of 2,5-Dimethyl-2,5-hexanediol and 6.32 g (0.062mole, 2.5 eq) of triethylamine in were dissolved 100 mL of dichloromethylene. Then 8.00 g (0. 076 mole, 3 eq) of methacryloyl chloride was added dropwise under cooling with ice water. The reaction was maintained overnight, washed with solution of potassium hydroxide (pH 8, 400 mL), subsequently washed with water three times and dried with magnesium sulfate, and the filtrated concentrated under reduced pressure. The resulting solid was purified by flash chromatography, eluting with 9:1 DCM/hex to yield 1.0g, 14% yield of a colorless liquid product. The structure was confirmed by $^1\text{H-NMR}$: (300 MHz, CDCl_3) δ (ppm), 1.5 (s, 12H), 1.87 (m, 6H), 1.7 (m, 4H), 5.72-6.42 (m, 6H)

The same procedure for testing cross-linking properties was followed for this compound. However, due to its high vapor pressure at room temperature, it evaporated from the wafer after spin coating, and later tests could not be performed.

2.11 Conclusion

The high cross linking behavior of (meth)acrylates make them good candidates for photoresist materials. Acrylates have a rapid curing process upon radical-initiated polymerization. A series of negative tone molecular resists with (meth)acrylate moiety was studied in this chapter. These compounds were either synthesized in the lab, or purchased. Thermal curing in suitable organic solvent (MIBK or MeOH) was investigated. In order to achieve high patterning resolution, the goal was to have a film that does not change in thickness at the curing temperature. The film thickness of the studied compounds was measured at room temperature, 70°C, 90°C, and 130°C.

Several deficiencies were observed in using acrylate compounds. Loss of film thickness was seen in all of the studied acrylates at curing temperatures, which was attributed to the acrylate shrinkage during crosslinking. Another observed problem was auto thermal polymerization at curing temperatures. Therefore, auto-thermal polymerization was studied for several acrylate compounds with different backbones and different numbers of functional groups. Auto thermal polymerization was observed for all of the tested compounds, which proved to be a major obstacle in using the studied acrylate compounds as resist materials.

Based on our findings, acrylate is not the suitable functional group for our applications. In the next chapter, epoxide and oxetane functional groups are investigated as crosslinking agents.

2.12 References

- (1) Plante, A.; Palato, S.; Lebel, O.; Soldera, A. *Journal of Materials Chemistry C* **2013**, *1*, 1037.
- (2) Montague, M. F.; Hawker, C. J. *J. Chem. Mater.* **2007**, *19*, 526.
- (3) Stroehriegl, P.; Grazulevicius, J. V. *Advanced materials* **2002**, *14*, 1439.
- (4) Matsukawa, D.; Okamura, H.; Shirai, M. *Polymer International* **2009**, *59*, 263.
- (5) Long, B. K.; Keitz, B. K.; Willson, C. G. *Journal of Materials Chemistry* **2007**, *17*, 3575.
- (6) B. D. Gates; Q. Xu, M. S.; D. Ryan; Willson, C. G.; Whitesides, G. M. *Chem. Rev.* **2005**, *105*, 1171.
- (7) M. Stewart; S. Johnson; S. V. Sreenivasan; Resnick, D.; Willson, C. G. *J. Microlithogr., Microfabr., Microsyst.* **2005**, *4*, 1.
- (8) Resnick, D. J.; Sreenivassan, S. V.; Willson, C. G. *Mater. Today* **2005**, *8*, 34.
- (9) Themistou, E.; Patrickios, C. S. *Macromolecules* **2006**, *39*, 73.
- (10) Pabin-Szafko, B.; Wisniewska, E.; Czech, Z. *CHEMISTRY & CHEMICAL TECHNOLOGY* **2009**, *3*.
- (11) K., M.; T., D. *Handbook of radical polymerization*; Wiley - Interscience, 2002.
- (12) G., O. *Principles of polymerization*; 3rd ed.; Wiley: New York **1991**.
- (13) Seto, R.; Sato, T.; Kojima, T.; Hosokawa, K.; Koyama, Y.; Konishi, G.-I.; Takata, T. *Journal of Polymer Science Part A: Polymer Chemistry* **2010**, *48*, 3658.
- (14) Hsiao, S.-H.; Yang, C.-P.; Lin, W.-L. *Macromol. Chem. Phys.* **1999**, *200*, 1428.
- (15) Korshak, V. V.; Vinogradova, S. V.; Vygodskii, Y. S. *J. Macro-mol. Sci.-Rev. Macromol. Chem.* **1974**, *C11*, 45.
- (16) Kawasaki, S.; Jin, F.; Takata, T. In *Metal, Ceramic and Polymeric Composites for Various Uses*; Cuppoletti, D. J., Ed. **2011**, *18*, 358.
- (17) Yang, C.-P.; Cheng, J.-M.; Hsiao, S.-H. *Makromol. Chem.* **1992**, *193*, 445.
- (18) Yang, C.-P.; Lin, J.-H. *J. Polym. Sci., Part A: Polym. Chem.* **1993**, *31*, 2153.

- (19) Yang, C.-P.; Lin, J.-H. *J. Polym. Sci., Part A: Polym. Chem.* **1994**, *32*, 2653.
- (20) Park, K. H.; Tani, T.; M. Kakimoto; Imai, Y. *Macromol. Chem. Phys.* **1998**, *199*, 1029.
- (21) Jian, Y.; He, Y.; Jiang, T.; Li, C.; Yang, W.; Nie, J. *Journal of Polymer Science Part B: Polymer Physics* **2012**, *50*, 923.
- (22) Fahem, Z.; Bauhofer, W. *Organic Electronics* **2012**, *13*, 1382.
- (23) Nichols, F. S.; R.G. Flowers *Ind. Eng. Chem.* **1950**, *42*, 292.
- (24) M.P. Patel; Braden, M.; Davy, K. W. M. *Biomaterials* **1987**, *8*, 53.
- (25) Venhoven, B. A. M.; Gee, A. J. D.; Davidson, C. L. *Biomaterials* **1993**, *14*, 871.
- (26) Ali, M. A.; Ooi, T. L.; Salmiah, A.; Ishiaku, U. S.; Ishak, Z. A. M. *Journal of Applied Polymer Science* **2001**, *79*, 2156.
- (27) McClelland, G. M.; Hart, M. W.; Rettner, C. T.; Best, M. E.; Carter, K. R.; Terris, B. D. *Applied Physics Letters* **2002**, *81*, 1483.
- (28) Ratnam, C. T.; Nasir, M.; Baharin, A.; Zaman, K. *Journal of Applied Polymer Science* **2001**, *81*, 1926.
- (29) Shirai, M.; Mitsukura, K.; Okamura, H. *chem. Mater.* **2008**, *20*, 1971.
- (30) Gerbaldi, C.; Nair, J. R.; Meligrana, G.; Bongiovanni, R.; Bodoardo, S.; Penazzi, N. *Journal of Applied Electrochemistry* **2009**, *39*, 2199.
- (31) Nair, J.; Gerbaldi, C.; Meligrana, G.; Bongiovanni, R.; Bodoardo, S.; Penazzi, N.; Reale, P.; Gentili, V. *J Power Sources* **2008**, *178*, 751.
- (32) Decker, C. *Prog Polym Sci.* **1996**, *21*, 593.
- (33) Okamura, H.; Terakawa, T.; Shirai, M. *Research on Chemical Intermediates* **2009**, *35*, 865.
- (34) Tesero, G. C.; Sastri, V. *J. Appl. Polym. Sci.* **1990**, *39*, 1425.
- (35) Sastri, V.; Tesero, G. C. *J. Appl. Polym. Sci.* **1990**, *39*, 1439.
- (36) Ogino, K.; Chen, J.-S.; Ober, C. K. *Chem. Mater.* **1998**, *10*, 3833
- (37) Tesoro, G. C.; Sastri, V. *J. Appl. Polym. Sci.* **1990**, *39*, 1425.

(38) Buchwalter, S. L.; Kosbar, L. L. *J. Polym. Sci., Part A: Polym. Chem. Mater.* **1996**, *34*, 1439.

(39) Yang, S.; Chen, J.-S.; Korner, H.; Breiner, T.; Ober, C. K.; Poliks, M. *Chem. Mater.* **1998**, *10*, 1475.

CHAPTER 3-SYNTHESIS AND CHARACTERIZATION OF CALIX[4]RESORCINARENE AND ITS DERIVATIVES

3.1 Introduction

Calixarenes are macrocyclic compounds that have received great attention in the fields of host-guest chemistry¹⁻³ non-linear optics⁴ and in HPLC stationary phases. Different calixarene derivatives have been synthesized and chemical modifications of them have been explored in literature⁵. Recently, calixarenes have received further attention as photoresist materials for high-resolution lithography¹. Great characteristics such as molecular sizes, good film forming properties, being curable with UV or electron beam, having high Tg, and good thermal stability make them good candidates for photoresist applications⁶⁻⁸. This kind of structure has attracted attention as an alternative core for polymeric resists, because of its great potential to lower line edge roughness (LER) and achieve high resolution patterning. Fujita *et al.* studied acetate derivatives of p-methylcalix[6]arene and found that they have ultrahigh resolution in e-beam lithography as negative tone resist⁶. Ueda *et al.* studied calix[4]resorcinarene, and reported the synthesis of octakis-O-tert-butyl carboxylated C-hexylcalix[4]resorcinarene and its derivatives as a positive tone photoresist⁹.

From the literature review, it could be proposed that calixarenes could be used as new starting materials for the synthesis of high performance UV and e-beam curable materials with a high Tg. We synthesized negative type molecular resists based on calix[4]resocinarene and functionalized them with epoxy or oxetane group.

3.1.1 Calixarene Structure

Calixarenes have phenolic units connected by methylene bridges to form different macrocyclic compounds. In 1872 Adolph von Baeyer, one of the great organic chemists in the nineteenth century and recipient of the 1905 Nobel Prize in Chemistry, reported the reaction of phenol with aldehydes in the presence of strong acids¹⁰. Resorcinol was the phenolic compound that Baeyer used in his investigations, and he discovered that it reacts with aldehydes such as acetaldehyde and benzaldehyde under acidic conditions, to produce a red colored product. The product was crystalline, and had a high melting point. At that time, he was looking for dye-stuff properties of the product. This compound did not have the desired properties for his application, so he decided not to continue further. About 10 year later, Michael¹¹ pursued this reaction and successfully isolated a pair of crystalline materials which he assumed were cyclic dimeric structures. In 1940, Niederl and Vogel¹² found that the molecular weight of the isolated product from the reaction of resorcinol is a good representative of cyclic tetramers^{13,14}. They performed several condensation reactions between aliphatic aldehydes and resorcinol, and measured the molecular weight of the product. They found that the ratio between aldehyde and resorcinol to be 4:4¹³.

Alois Zinke suggested a cyclic tetrameric structure of the product phenolic compound and aldehydes in 1944¹⁵. He proposed that all four OH groups in his tetrol product were in the intraannular (“endo-annular”) position. Later, Niederl suggested that all eight OH groups in the product structure of resorcinol and aldehyde reaction were in extraannular (“exo-annular”) position¹⁰. (Figure 3.1)

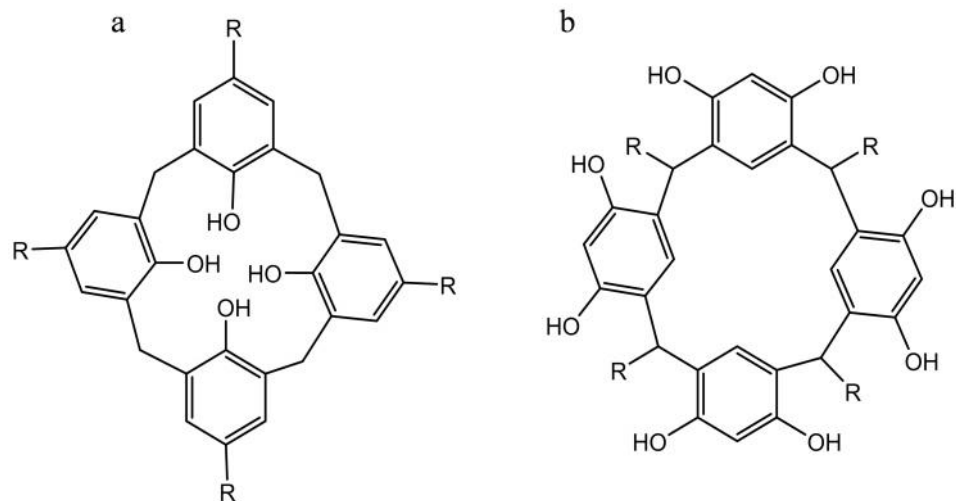


Figure 3.1. Calixarene compound with OH groups in intraannular (“endo-annular”) position (a), and in extraannular (“exo-annular”) position (b)

3.1.2 Nomenclature

In the late 1970s, David Gutsche named this type of compound as “calixarene”¹⁶. Calixarene is derived from the Greek name “calix”, meaning “vase”, and “arene”, indicating the presence of aromatic rings. In Figure 3.2, the space filling model of a cyclic tetramer (calixarene) and a vase that looks like the calixarene crater are shown.



Figure 3.2. Space-filing molecular model of a calixarene compound (left) and a vase (right)

Several calixarenes with different sizes have been synthesized. To distinguish between compounds, a bracketed number is positioned between *calix* and *arene* to indicate the number of phenolic units. These phenolic units are connected to each other by methylene bridge and form the cavity of the molecule. In Figure 3.3 calixarene compounds with different sizes are shown.

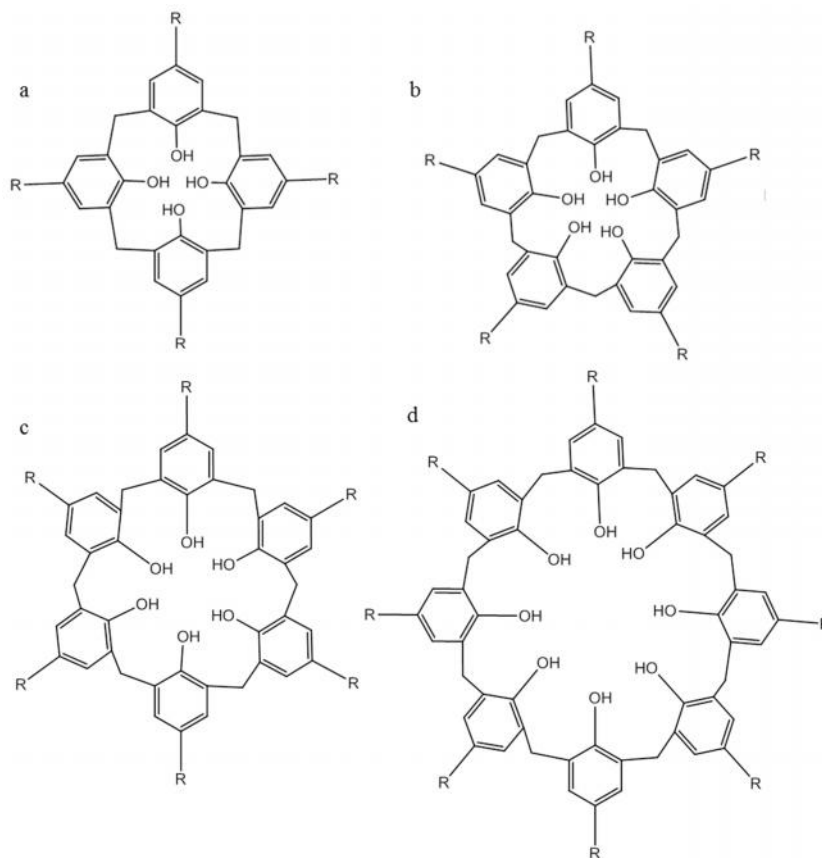


Figure 3.3. Different calixarene compounds: calix[4]arene (a), calix [5]arene (b), calix [6]arene (c), and calix [8]arene (d)

If the aromatic ring is modified with functional groups, the ring is specified with appropriate prefixes. For example, if resorcinol is used instead as phenolic compound, the name will be calix[n]resorcinarene. If a substituent is attached to methylene carbons of a calix[n]resorcinarene, it is indicated by a prefix “C-substituent”. For example, if

resorcinol and p-bromobenzaldehyde are reacted to make calixarene, the product's name is "C-p-bromophenyl calix[4]resorcinarene".

3.1.3 Calixarene Conformers

Calixarenes with different sizes and configurations have been synthesized¹⁰. Cyclic tetramers such calix[4]arenes have been investigated^{17,18}. Calix[4]arenes are not usually planar due to the presence of hydrogen bonding, which increases stability. Based on the conformation for the macrocyclic ring, the ring can adopt five symmetrical arrangements: crown (C_{4v}), boat (C_{2v}), chair (C_{2h}), diamond (C_s), and saddle (D_{2d}) conformations. Figure 3.4 shows these five conformers of calix[4]arenes based on ring orientation. Sometimes in the literature, these conformers are classified as four conformers such as cone (all "up"), partial cone (three "up" and one "down"), 1,2-alternate (two "up" and two "down"), and 1,3-alternate (two "up" and two "down")¹⁸.

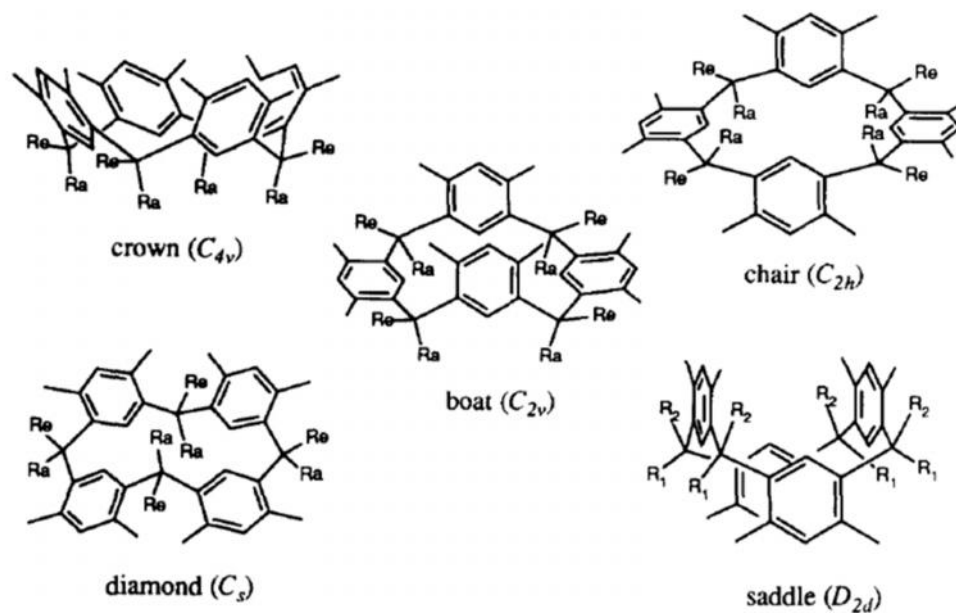


Figure 3.4. Five different conformers of calix[4]arenes based on ring orientation

There are four conformers of calix[4]arenes based on the substituent configuration at methylene bridges. As illustrated in Figure 3.5, four configurations are specified as cis-cis-cis (ccc), cis-cis-trans (cct), cis-trans-trans (ctt), and trans-cis-trans (tct).

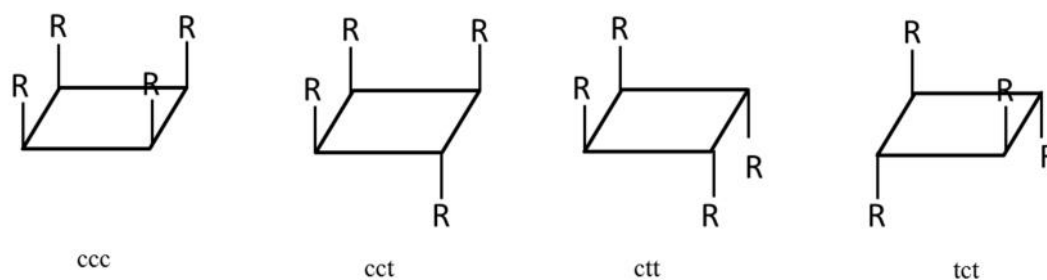


Figure 3.5. Four different conformers of calix[4]arenes (and calix[4]resorcinarene) based on substituents at the methylene bridges

By modifying the condensation reaction conditions and aldehyde structure, the distribution of the isomers can be controlled. Intramolecular hydrogen bond interactions and non-bonded steric hindrance play a part in determining the degree of conformational rigidity in these compounds. By crystallization, the flexibility of calixarenes can be controlled. The desired conformations can then be separated in the solid state upon crystallization. If calixarenes are functionalized with bulkier groups, rotations and the exchange between conformers is inhibited and leads to another way of controlling conformations.

Figure 3.6 shows the structure of the crown (ccc) conformer. The crown conformer is the thermodynamically most stable conformer, which is mainly obtained after long reaction times. Compared to other conformers, the crown conformer forms the maximum number of hydrogen bonds between the resorcinol units, while having the

minimum steric interference between the substituents at the methylene-bridge positions^{19,20}.

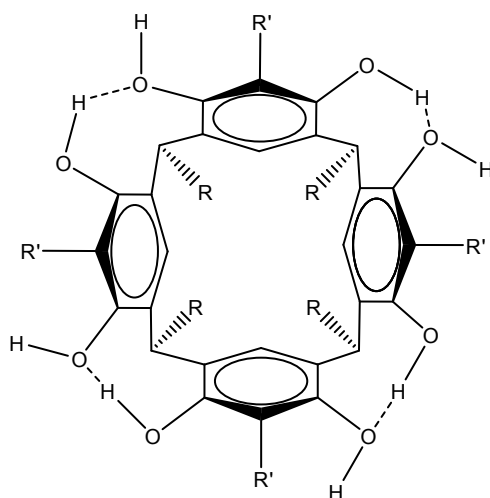


Figure 3.6. Crown conformer structure that has the maximum hydrogen bonding among conformers

The crown (ccc) conformer can convert to the boat conformer in solution at room temperature. In Figure 3.7, equilibrium reactions between boat and crown conformers are shown. The chair conformer can be synthesized as a side product, under kinetically controlled conditions. This conformer is finally converted to the crown conformer, which is thermodynamically more stable²⁰.

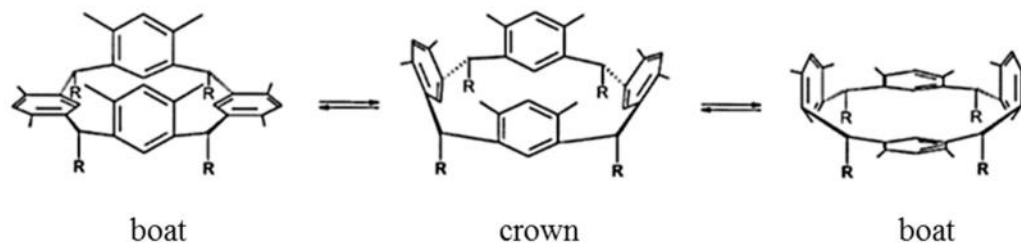


Figure 3.7. Boat and crown conformer conversions for calix[4]resorcinarene

Weinelt *et.al* quantitatively studied the isomerization of calix[4]resorcinarene conformers. They started the reaction with just the boat (and crown) conformer in a 5% HCl solution in methanol at 50°C. In Figure 3.8, the concentration of each of the conformers (boat, diamond, and chair) was monitored with time. Conversions reached equilibrium after approximately 1200 seconds. At equilibrium, about half of the boat conformers were converted to the chair and diamond conformers with the ratio of 1 to 4, respectively. At this temperature, the boat conformer was slightly more stable than diamond conformer. The chair conformer was also observed as the least thermodynamically stable conformer¹³.

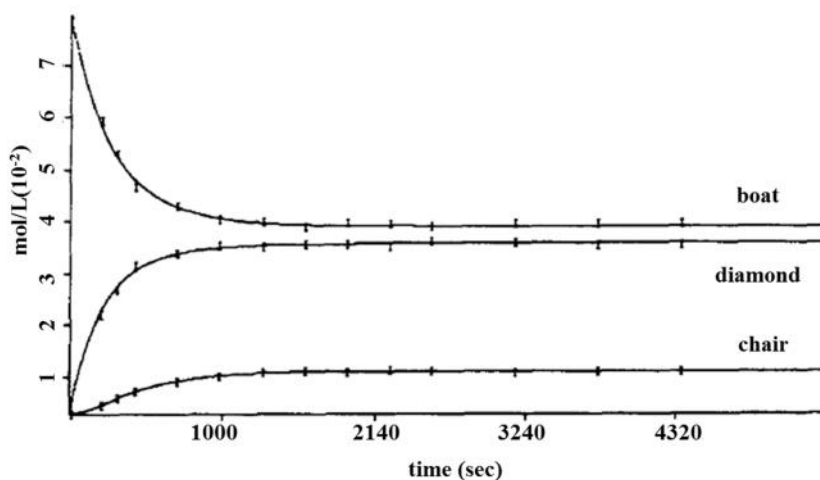


Figure 3.8. Concentration of calix[4]resorcinarenes conformers as a function of time, in 5% solution of HCl in methanol at 50°C

Conversion between conformations likely occurs when an aryl group rotates around the C-2/C-6 axis and it makes less hydrogen bonding. If larger groups are present, greater interference is expected for rotation¹⁸. Kondyurin *et al.* found that the chair (ctt) conformation occurs exclusively in the rigid conformation²¹. Therefore, a rigid

chair conformer with axial substituents does not easily convert into another conformer²¹. It is shown that as the size of the calixarene increases, its conformational mobility increases as well¹⁴. For example, calix[5]arene, has a coalescence point in dynamic ¹H-NMR studies at a considerably lower temperature than that of calix[4]arenes¹⁴. Surprisingly, calix[8]arenes show dynamic ¹H-NMR characteristics that are almost identical with calix[4]arenes in a non-hydrogen bonding solvents. This finding shows that the conformational rigidity of the calix[8]arene is primarily due to intramolecular hydrogen bonding.

3.2 Cationic Polymerization

Cationic polymerization is classified as a chain growth polymerization. In this polymerization, a cationic initiator is used which can be a protic acids²², a Lewis acid²³, carbenium ion²², or photoacid generator (PAG)s²⁴. PAGs are photoactive compounds which are used to produce acid upon to the radiation. PAGs are highly active initiators in cationic polymerization for various organic monomers such as epoxides and oxetanes (negative tone photoresist) and also to break the bond of acid sensitive functional groups such as tertiary esters (positive tone photoresists)²⁴.

Figure 3.9 shows general mechanism for cationic polymerization of epoxy and oxetane resists^{25,26} using PAGs as initiators. The reaction starts after irradiation with UV light and during the post exposure bake (PEB) to generate acid HX. In these systems acid produced by irradiation works as a catalyst to initiate cationic polymerization. The proton transfers to a monomer which activates the monomer. The reactive species will react with other monomers, and this process is propagated to form a polymer²³. In cationic polymerization, the photoacid is only active for one epoxy, or oxetane activation, and

after epoxide or oxetane is protonated, they work as active sites for further reaction and polymerization.

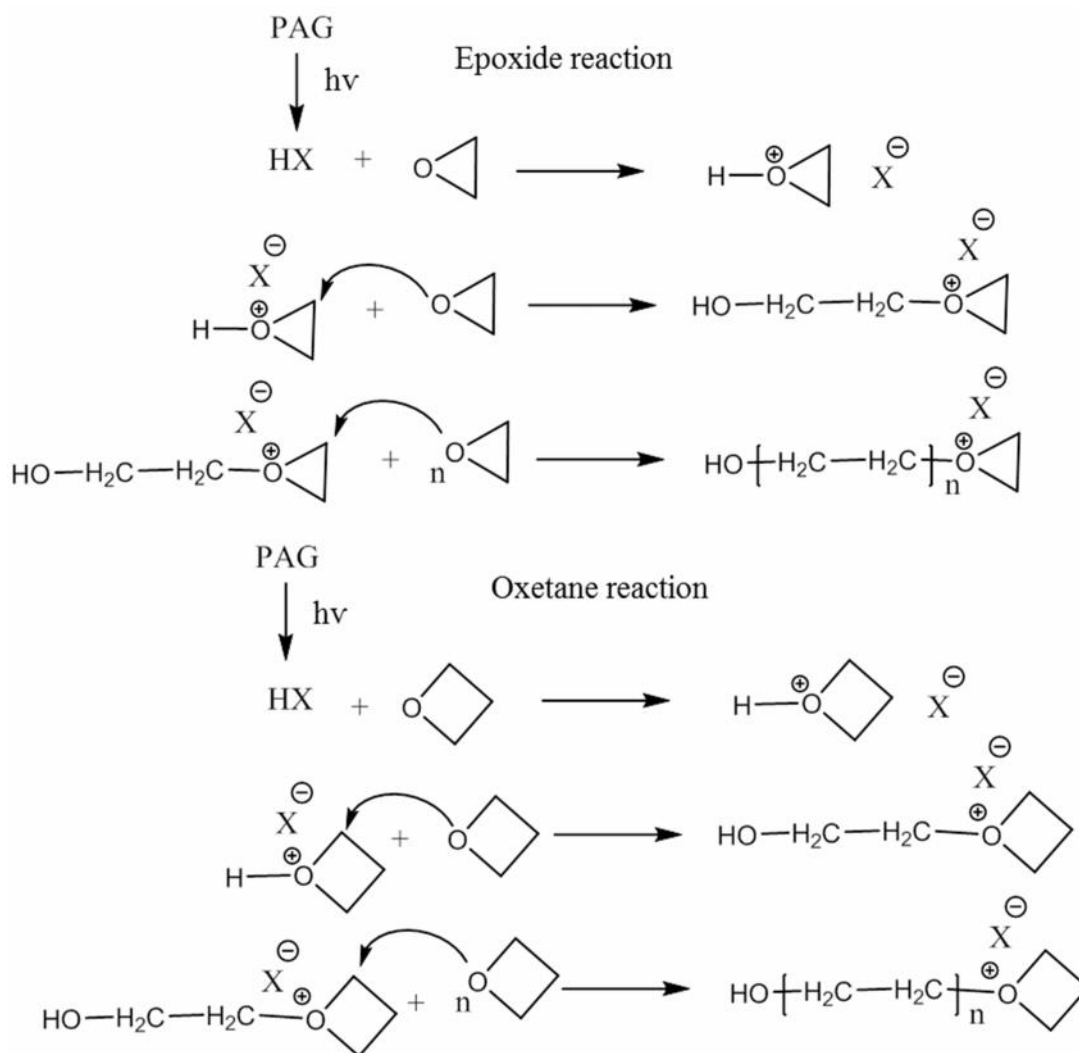


Figure 3.9. Cationic polymerization of epoxy and oxetane

Our goal in this study is to make compounds that can effectively developed for high resolution and improved LER²⁷. Our work in this chapter is focused on synthesizing molecular glass photoresists such as calix[4]resorcinanes fully functionalized with oxetane (C4MR-8x) and epoxide (C4MR-8Ep) moities to study as negative tone resists. The significant advantage of negative tone resists is to make high MW by creating highly

cross-linked structures for increasing mechanical strength. This could reduce swelling of the photoresist, which is a limiting factor for obtaining high resolution patterning.

In this chapter we synthesize and characterize calix[4]resorcinane (C4MR), C4MR-8Ox, C4MR-8Allyl and provide two pathways for synthesis of C4MR-8Ep.

3.3 Materials and Instruments

Unless otherwise noted, all reagents and solvents were purchased from Sigma-Aldrich, TCI America, or Alfa-Aesar and used as received. A Varian Mercury Vx 300 and Bruker 400MHz were used to collect NMRs. FTIR spectra were collected on a Bruker IFs66vS using KBr pellets. MALDI mass spectra were collected on an Applied Biosystems 4700 Proteomics Analyzer.

3.4 Synthesis of Calix[4]resorcinarenes (C4MR)

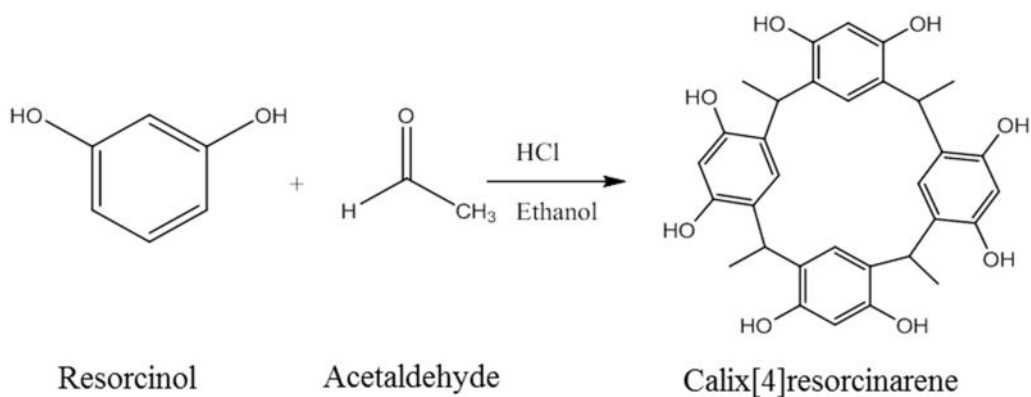


Figure 3.10. Synthesis route for making C4MR

The synthetic route for making C4MR is shown in Figure 3.10. In a 500 mL round bottom flask, a solution of resorcinol (16.5 g, 0.15 mol, 1 eq) and acetaldehyde (6.5 mL, 0.15 mol, 1 eq) in 150 mL of a 50 vol % aqueous ethanol solution was stirred and heated at 75 °C. Concentrated hydrochloric acid (37.7 mL, 1.21 mol, 8 eq) was added dropwise. The reaction mixture was continuously stirred at 75°C. After 1 h, the mixture was cooled with an ice bath, and a precipitate was collected with a sintered-glass filter and dried under reduced pressure. The filtrate was evaporated, and the second precipitate was filtered. The collected precipitate was recrystallized from a 50 vol % aqueous ethanol solution to yield 4.5 g (22%) of a colorless solid. The product was characterized by ¹H-NMR, IR and MALDI. ¹H-NMR (300 MHz, DMSO-d₆): CH₃ (1.28, d,), CH (4.36, m), aromatic CH (6.13, s), aromatic CH (6.75, s), OH (8.52, br). IR (KBr): 3100-3700 (OH), 1600 (C=C of aromatic) 1465 (CH₂ bend) 1379 (CH₃ bend) 1140-1215 (C-O-C). MALDI spectrometry shows the signal at m/z 544.14.

The mechanism for synthesizing C4MR is shown in Figure 3.11.

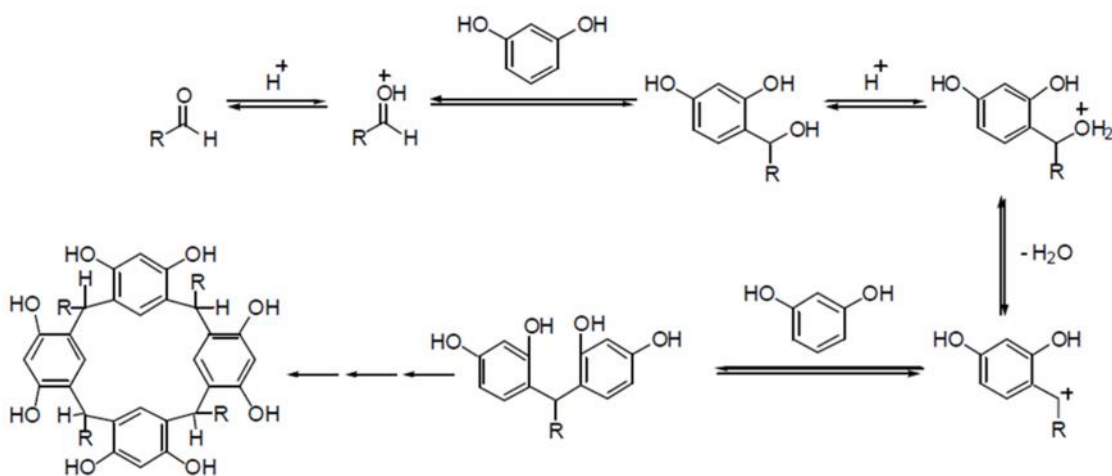


Figure 3.11. Mechanism for synthesizing of C4MR ²⁸

3.5 Synthesis and Characterized Fully Functionalized C4MR

A general procedure for making a functionalized C4MR is a substitution reaction using the phenolic oxygen of C4MR. Functionalized C4MR compounds have been synthesized by substitution reaction with 3-(chloromethyl)-3-methyloxetane, allyl bromide, and epibromohydrin (EBH) to give the corresponding ethers in the presence of inorganic strong bases and phase-transfer catalysis (PTC).

Phase-transfer catalysis (PTC) is utilized in reactions between anions and organic substrates. The mechanism of PTC reaction was first proposed in 1971^{29,30}. PTC is needed for anions and organic substrates, due to the solubility issues. Many anions are soluble in water but insoluble in organic solvents. However, organic reactants are mostly soluble in organic solvents and not water. In such systems, the catalyst can act as a transfer agent by extracting the anion from the aqueous or solid phase into the organic phase or in the interfacial region, where the anion and organic reactants can readily react.

In Figure 3.12, the proposed mechanism for phase transfer catalysis is shown. The catalyst is often a quaternary ammonium salt (e.g., tetrabutyl ammonium), so the phase transfer compound is often noted as Q^+ . The ion pair Q^+X^- (X^- is anion) is a much looser ion pair than, say, Na^+X^- . This weakness of the ion pair leads to increased reactivity. After the catalyst transfers the anion to the organic phase, the anion goes through a nucleophilic substitution reaction with the organic reagent. At the end of the reaction, the phase transfer catalyst usually transfers the leaving group (anion Y^-) back to the aqueous or solid phase. This makes it easier to separate the by-product from product.

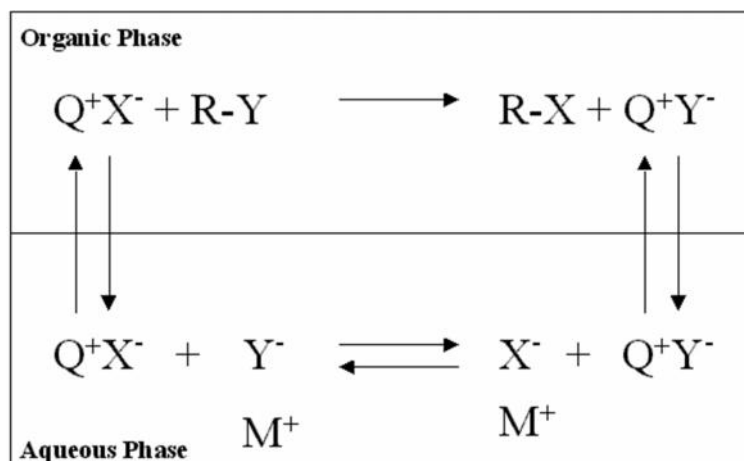


Figure 3.12. Mechanism of phase-transfer catalysis ²⁹

3.5.1 Synthesis of C4MR-8Ox

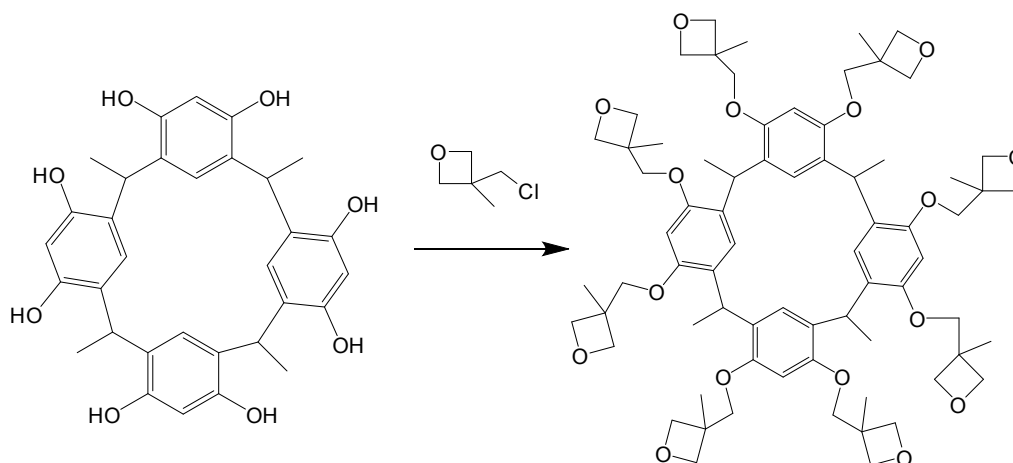


Figure 3.13. Synthesis reaction of C4MR-8Ox

The synthetic route for making C4MR-8Ox is shown in Figure 3.13. C4MR (0.980 g, 1.8 mmol, 1 eq) and Na_2CO_3 (6.105 g, 57.6 mmol, 32 eq) were dissolved in *N*-methyl-2-pyrrolidone (NMP; 3 mL) at room temperature under stirring, and 3-(chloromethyl)-3-methyloxetane (6.94 g, 57.6 mmol, 32 eq) and tetrabutylammonium

bromide (TBAB) (3.6 g, 3.6 mmol, 2 eq) were added to the solution. The mixture was stirred at 100 °C for 24 h. The reaction mixture was diluted with chloroform and washed three times with water. The chloroform solution was dried overnight with anhydrous Na₂CO₃ and filtered. The chloroform was evaporated *in vacuo*, and the precipitate from a acetonitrile/ chloroform mixed solvent was dried at 60 °C for 24 h *in vacuo*. The yield of reaction was 0.500 g (22%). The product was characterized by ¹H-NMR, IR and MALDI. ¹H-NMR (300 MHz, CDCl₃), 1.20 (s, 12H), 1.42 (d, 12H), 1.44 (s, 12H), 3.48 (m, 4H), 3.78 (d, 4H), 4.12-4.49 (m, 26H), 4.48 (m, 4H), 4.62 (m, 4H), 6-7.29 (m, 8H). IR (KBr): 2800-2950 (C-H stretch), 1600 (C=C of aromatic) 1465 (CH₂ bend) 1379 (CH₃ bend) 1140-1215 (C-O-C). MALDI spectrometry shows signal at m/z 1216.6.

3.5.2 Synthesis of C4MR-8Allyl

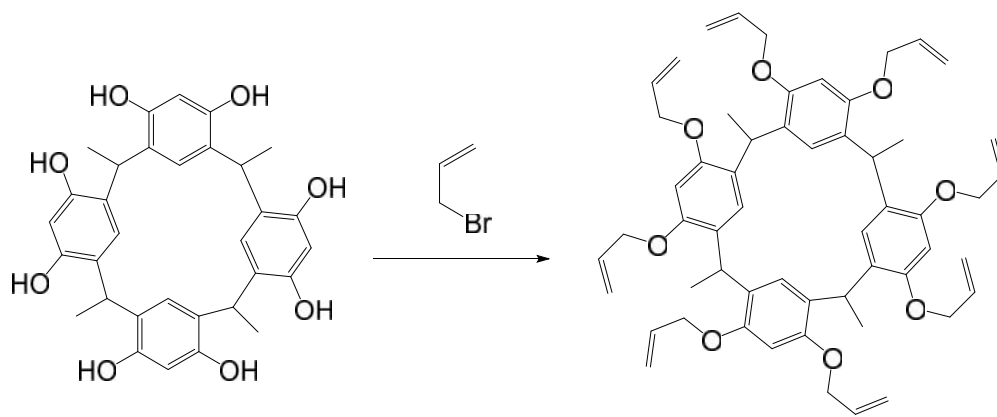


Figure 3.14. Synthesis reaction of C4MR-8Allyl

The synthetic route for making C4MR-8Allyl is shown in Figure 3.14. C4MR (2.18 g, 4 mmol, 1 eq) and K₂CO₃ (6.63 g, 48 mmol, 12 eq) were mixed in acetone at room temperature under stirring. Allyl bromide (5.81g, 48 mmol, 12 eq) and 18-crown-6 (0.93 g, 3.52 mmol, 0.88 eq) were added to the solution. The mixture was heated under

reflux for four days under vigorous stirring. The reaction mixture was poured in 200 mL water and the solid precipitation was collected. The obtained solid was crystallized in isopropanol alcohol and the product was dried at 60 °C for 24 h in vacuum to obtain 1.65g of a colorless solid (47% yield). The product was characterized by $^1\text{H-NMR}$, IR and MALDI. $^1\text{H-NMR}$ (400MHz) at room temperature shows a very broad peak at aromatic region. IR (KBr): 2800-2950 (C-H stretch), 1600 (C=C of aromatic) 1465 (CH_2 bend) 1379 (CH_3 bend) 1140-1215 (C-O-C). 990 (C-H bend). MALDI spectrometry shows signal at m/z 864.5. Melting point is 151-152°C

3.5.2.1 Variable-temperature NMR studies on C4MR-8Allyl

The dynamic behavior of C4MR-8Allyl in solution has been studied by $^1\text{H-NMR}$ (400MHz) in the -70°C to 65°C temperature range. Figure 3.15 shows $^1\text{H-NMR}$ of this compound at room temperature. Interestingly, the $^1\text{H-NMR}$ spectrum of C4MR-8Allyl shows a very broad peaks in aromatic region and also a broad peak in ($\text{CH}_2\text{-CH=CH}$) region at room temperature in NMR time scale.

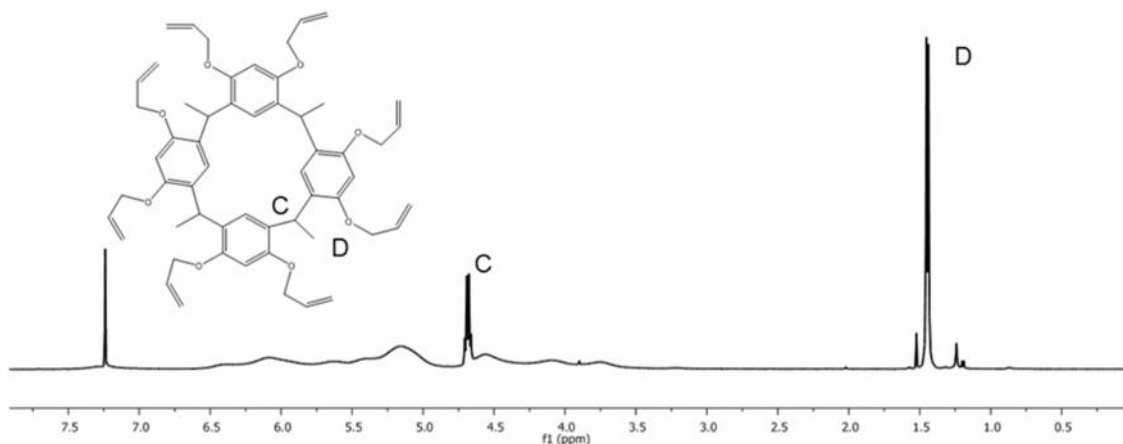


Figure 3.15. $^1\text{H-NMR}$ (400 MHz) spectra of C4MR-8Allyl in CDCl_3 at RT.

Peak-broadening in the spectrum might be due to the presence of different conformers in solution on the NMR time scale. In the C4MR compound, the major driving force in having only one stable conformer is having intramolecular hydrogen bonds. However, this driving force is no longer available for C4MR-8Allyl¹⁹. If different possible conformers (based on conformational exchanges of macrocycle) were present in solution, the NMR peaks would be broad. In this case, every conformer would give a single line resonance in aromatic region (5-6.5 ppm) and a broad peak would be observed. Since the exchange between conformers is rapid on the NMR time scale, it cannot be determined which conformer predominates at the room temperatures. Figure 3.16 shows common conformers of calix[4]resorcinarene.

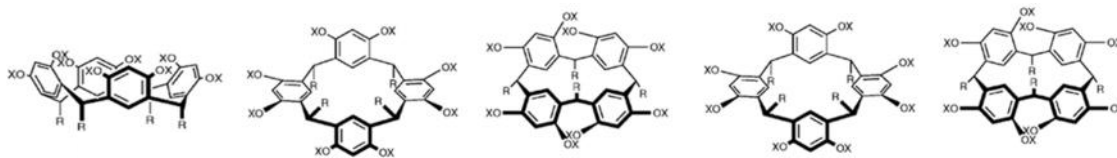


Figure 3.16. Common conformers of calix[4]resorcinarene¹⁸

For the allyl group, we also see peak broadening, because each functional group can have a different position with respect to the macrocyclic ring in each conformer. As a result, a broad peak (3-4.5ppm) is seen for allyl and vinyl hydrogens.

In Figure 3.17, the ¹H-NMR spectra of C4MR-8Allyl are shown at 45°C, 55°C, and 65°C. By raising the temperature to 45°C and above, the peaks that correspond to the phenyl CH and allyl group were still broad. At high temperature the exchange between conformers were even quicker than at room temperature on the NMR time scale, and caused peak broadening

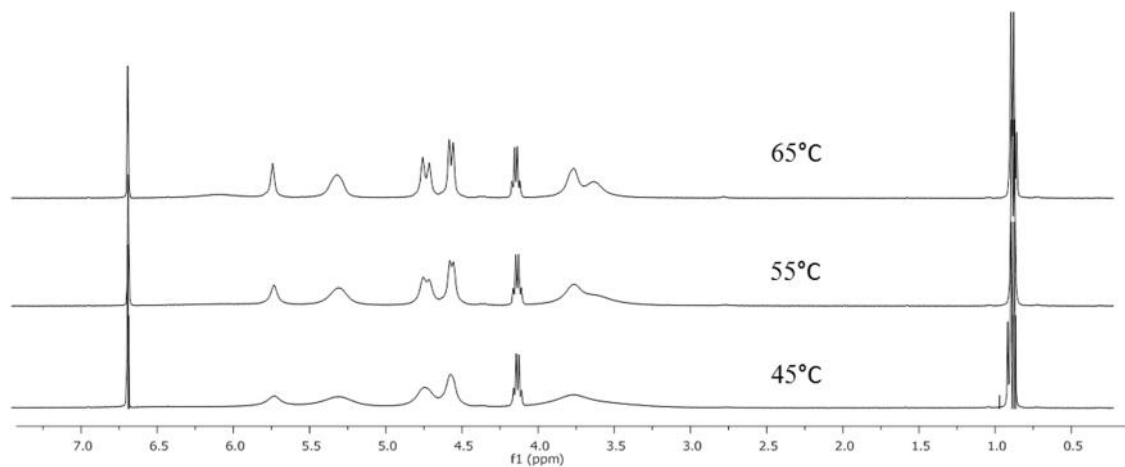


Figure 3.17. $^1\text{H-NMR}$ (400 MHz) spectra of C4MR-8Allyl in CDCl_3 at 45, 55, and 65°C

In Figure 3.18, the $^1\text{H-NMR}$ spectra of C4MR-8Allyl is shown at -70°C , -46°C , and -23°C . When the solution of C4MR-8Allyl in CDCl_3 was cooled to -70°C , the allylic and vinylic ($\text{CH}_2\text{-CH=CH}_2$) peaks, and the peaks in aromatic region became sharp, and then split into several peaks. Peaks for these regions were broad at room temperature.

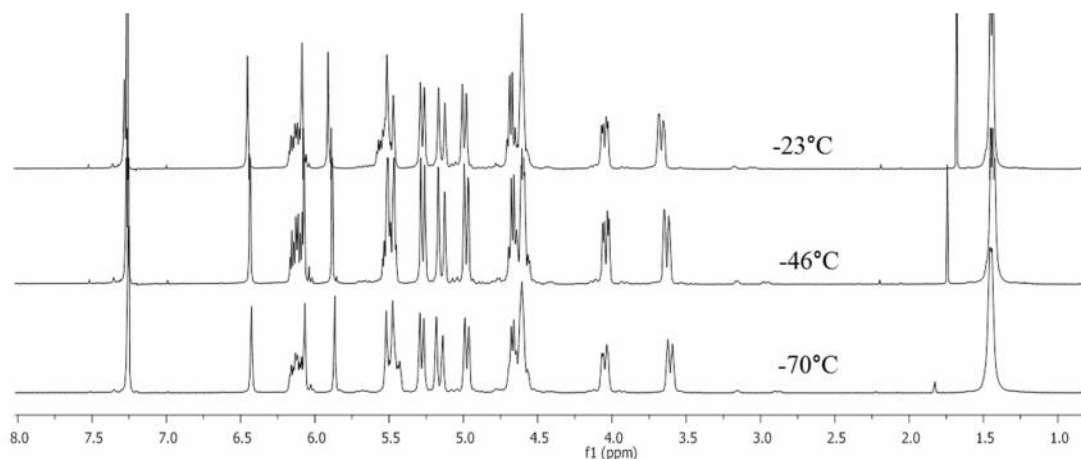


Figure 3.18. $^1\text{H-NMR}$ (400 MHz) spectra of C4MR-8Allyl in CDCl_3 at -70°C , -46°C , and -23°C

At -70°C , bond rotations might freeze and restrict the interchange between isomeric states (conformers). Therefore, the very broad peak of the CH in aromatic

region at room temperature turned to three separated peaks at -70°C . This shows that hydrogens in the aromatic region are not magnetically equivalent.

From Figure 3.18, it can also be inferred that OCH_2 (allylic proton) group are not magnetically equivalent⁵ at -70°C . This is also attributed to the restricted rotation of the bonds. The CH_2 of the allylic groups shows three separate peaks at -70°C that might be due to different positions of allyl in regard to inside or outside of aryl field. Some CH_2 that are on high field in NMR spectrum can be assigned as being “inside” of the aryl moiety and shielded by it. This effect is due to the anisotropy associated with π -electron aromatic systems. In such systems, the π electrons interact with the NMR applied field which induces a magnetic field. As a result, the nearby protons experience 3 different fields, including the applied NMR field, the shielding field from valence electrons and the field due to the π system. Depending on the position of the proton, it can be either shielded or deshielded. Low field chemical shift is attributed to the CH_2 that is “outside” of aryl moiety and deshielded. High field chemical shift is attributed to the CH_2 that is “inside” of aryl moiety and is shielded³¹.

Assignment of the signals for C4MR-8Allyl was further studied with two-dimensional ^1H - ^1H COSY NMR spectra. Figure 3.19 shows the COSY NMR for C4MR-8Allyl at -70°C . The two-dimensional COSY (COrrrelation SpectroscopY) experiment helps in determining the connectivity of a molecule by revealing which protons are spin-spin coupled.

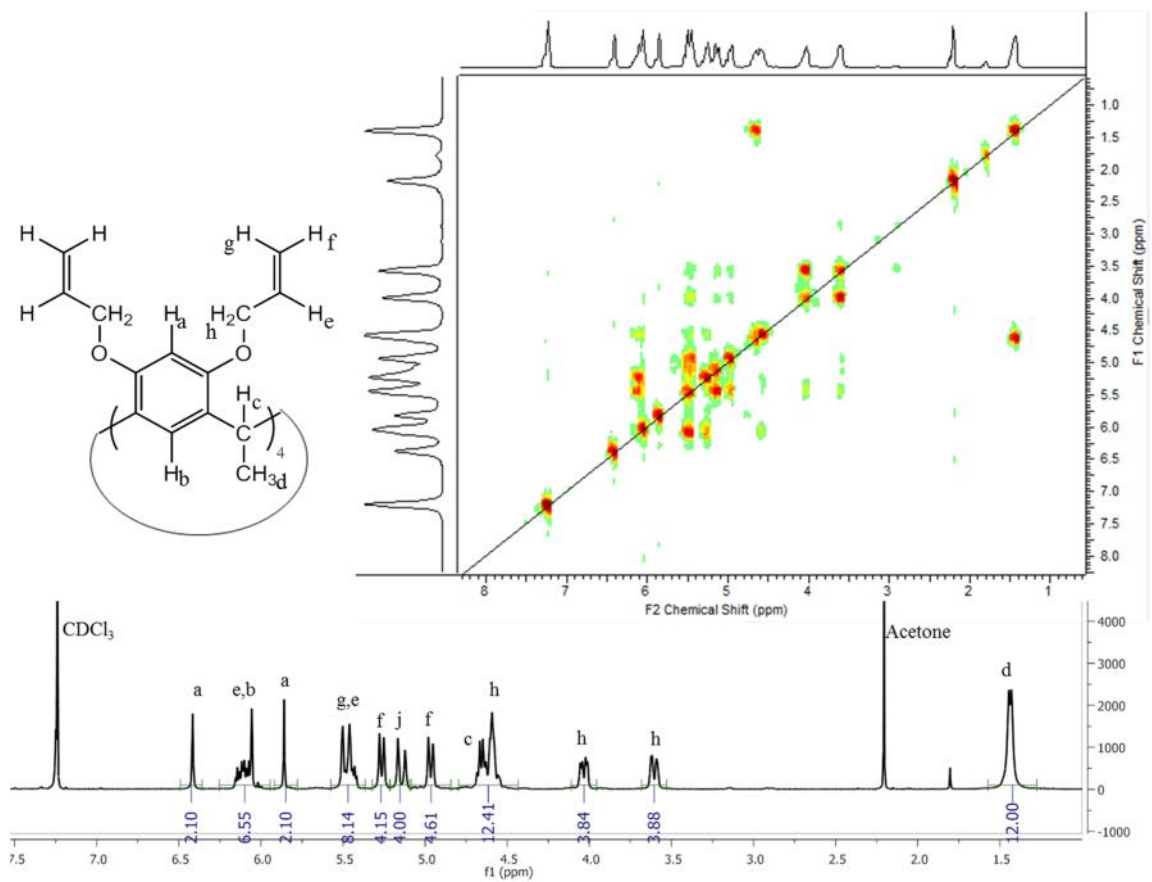


Figure 3.19. ^1H - ^1H COSY NMR spectrum of C4MR-8Allyl in CDCl_3 at -70°C and peak assignment

3.5.2.2 Conformational behavior

The $^1\text{H-NMR}$ 400 MHz spectrometer was calibrated with pure MeOH (for low temperature from -70°C to -23°C) and with pure ethylene glycol (for 45°C to 65°C)³². At the lowest studied temperature (-70°C), there were three singlets [5.86 (1H), 6.06 (2H), 6.42 (1H)] that might indicate the presence of the partial cone conformation³³. By increasing temperature, this conformer exchanged with other conformers, resulting in a mixture. Figure 3.20 shows $^1\text{H-NMR}$ of C4MR-8Allyl at different temperatures. Looking at NMR spectra from -70°C to 65°C , the first coalescence temperature was observed at 21°C . At this temperature, the two signals for macrocycle just merged. This coalescence behavior resulted from the equilibrium between partial cone and other conformers. The peaks that corresponded to the vinyl hydrogens also merged at 21°C and are shown in Figure 3.20

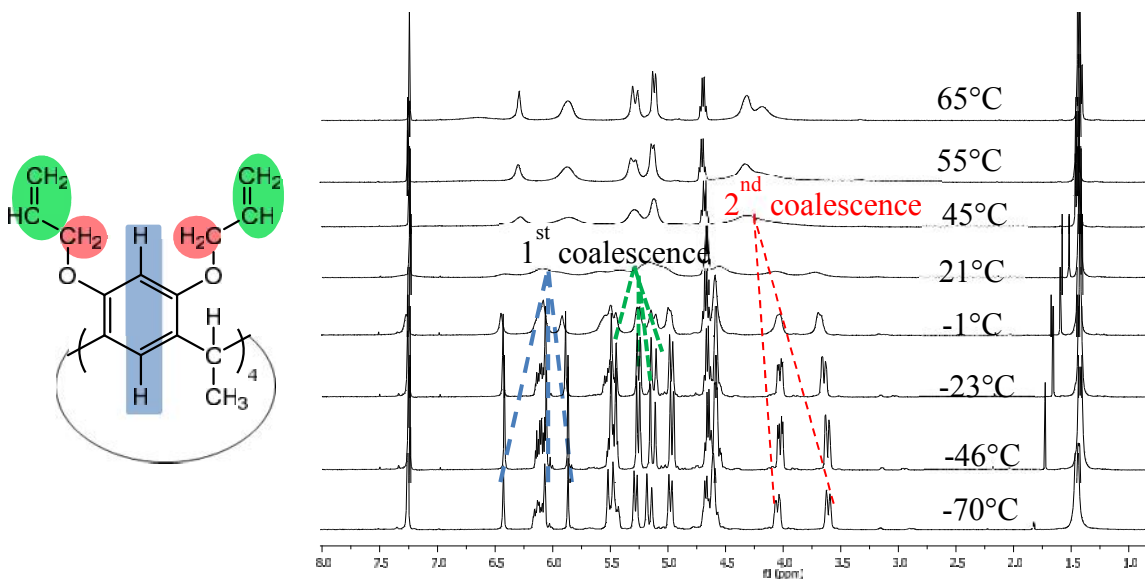


Figure 3.20. $^1\text{H-NMR}$ for C4MR-8Allyl at different temperatures

From the coalescence temperature, Gibbs free energies (ΔG^\ddagger) can be calculated for the exchange process by using equation 3.1 and 3.2³⁴.

$$k_{Tc} = \frac{\pi\sqrt{\Delta\nu^2 + 6j^2}}{\sqrt{2}} \quad 3.1$$

Where k_{Tc} is the rate constant (s^{-1}), T_c is the coalescence temperature (K), and $\Delta\nu$ is the difference in the chemical shifts (Hz) and j is the spin-spin splitting (Hz). In equation 3.2, the rate constant is shown using the Eyring relation. ΔG^\ddagger can be calculated using this equation.

$$k_{Tc} = \kappa \frac{k_B T_c}{h} e^{-\Delta G^\ddagger / RT} \quad 3.2$$

Where h is Planck's constant ($1.584 \cdot 10^{-34}$ cal.s), k_B is the Boltzmann constant ($3.2998 \cdot 10^{-24}$ cal/K), R is the universal gas constant (1.9872 cal/(K.mol)) and κ is the transmission coefficient which is 1.

From the first coalescence, ΔG^\ddagger is determined to be about 57.4 KJ/mol for the conformational exchange process at 21°C. As the temperature is increased above 21°C, the second coalescence occurs to the doublets [3.60 (0.9H) and 4.03 (0.9H)]. The second coalescence behavior might correspond to the conformational exchange of CH₂ of allylic group. From the second coalescence, Gibbs free energy (ΔG^\ddagger) was determined as 62.1 KJ/mol for the conformational exchange at 45°C.

The NMR data (Figure 3.21) indicates that conformational exchanges of macrocyclic ring happens slowly on the NMR time scale at low temperatures below 21°C. The first coalescence happens close to 21°C. As the temperature is raised to 45°C, the second coalescence that corresponds to the allylic group occurs. By increasing the

temperature further, the observed broad peak for allylic group converts to two broad peaks

3.5.3 Synthesis of C4MR-8Ep

We synthesized C4MR-8Ep with two different methods. The first method is by epoxidation of C4MR-8Allyl. This method's advantage is in allowing better reaction control, and having the reaction temperature under the room temperature, which avoids epoxide polymerization. The second method is functionalizing C4MR using epibromohydrin. In this section, we compare these two synthesis methods.

3.5.3.1 Synthesis of C4MR-8Ep from C4MR-8Allyl

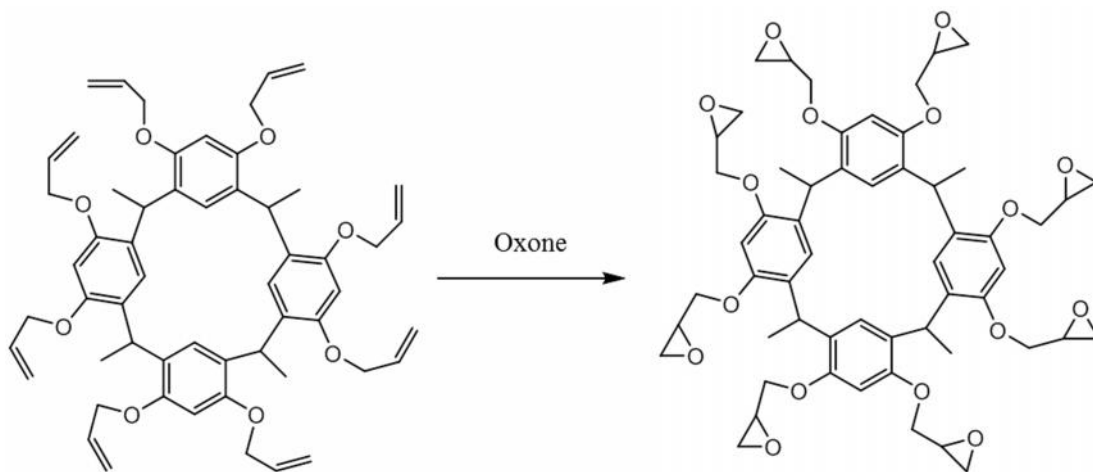


Figure 3.21. Catalytic epoxidation of C4MR-8Allyl with oxone for C4MR-8Ep synthesis

One of the efficient methods for the catalytic epoxidation of alkenes is using peroxomonosulfate (Oxone). Oxone is stable at room temperature, is low cost and non-toxic. Oxone is soluble in water, and it can be removed after reaction by washing the

product with water. Figure 3.21 shows the catalytic epoxidation of C4MR-8Allyl with Oxone for C4MR-8Ep synthesis.

The reaction mechanism for this synthesis includes making a dioxirane intermediate. In this process, dioxirane forms at the carbonyl carbon by nucleophilic attack of Oxone. Subsequently, potassium hydrogen sulfate is formed³⁵. The next step in the mechanism is oxygen transfer to the double bonded carbon to form the epoxy product. This step also regenerates the initial ketone. Figure 3.22 shows the reaction mechanism of epoxidation of carbon carbon double bond.

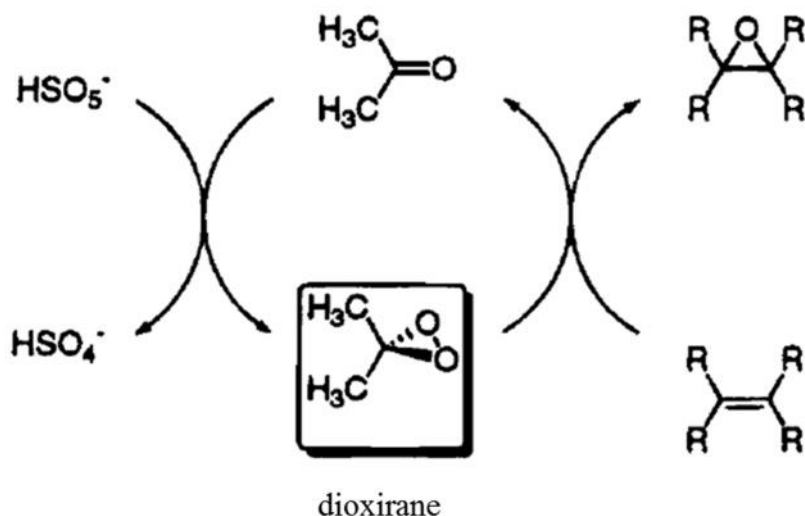


Figure 3.22. Reaction mechanism of epoxidation of carbon-carbon double bond

Synthesis procedure

C4MR-8Allyl (0.4 g, 0.46 mmol, 1 eq) and NaHCO_3 (3.5g, 41 mmol, 24 eq) were dissolved in acetone and CH_2Cl_2 at ice bath temperature under stirring. Oxone ($2\text{KHSO}_5 \cdot \text{KHSO}_4 \cdot \text{K}_2\text{SO}_4$, 9.1 g, 14.8 mmol, 8 eq) in water (26 mL) was added dropwise to a vigorously stirred mixture. The mixture was stirred at room temperature for 24 h. The epoxidation procedure was repeated 4 times until the aryl allyl ether was fully

converted to glycidyl ether. The solution was washed three times with water, dried overnight with anhydrous Na_2CO_3 , and filtered. The solution was evaporated. A yellow solid product 20mg precipitated from the methanol and was dried for 24 h in vacuum. ^1H NMR: (300 MHz, CDCl_3): 1.44 (d, 3.0H), 2.40–3.05 (m, 4.0H), 3.24–4.42 (m, 6.0H), 4.63 (m, 1.0 H), 5.80–6.75 ppm (m, 2.0H).H).

3.5.3.2 Synthesis of C4MR-8Ep using epibromohydrine

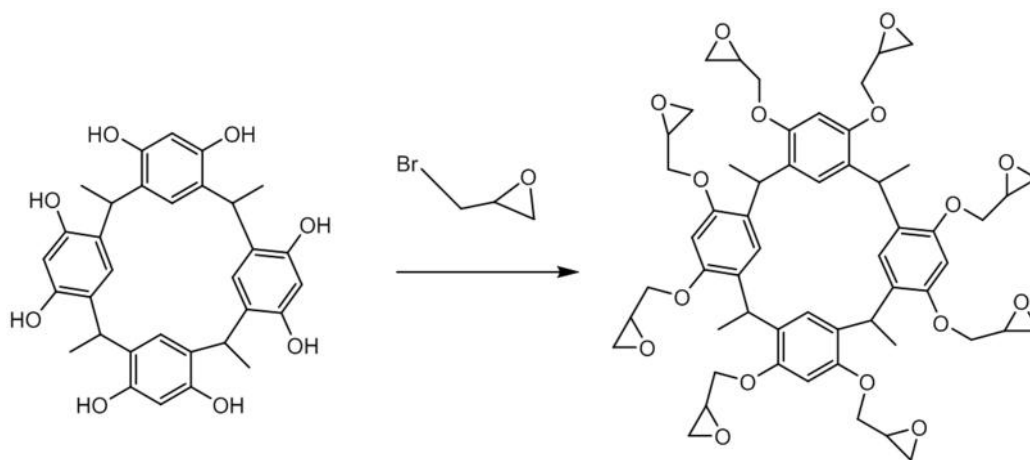


Figure 3.23. Reaction synthesis of C4MR-8Ep by functionalizing C4MR using epibromohydrine.

The synthetic route for making C4MR-8Ep is shown in Figure 3.23. C4MR (1.089 g, 2 mmol, 1 equiv.) and K_2CO_3 (8.845, 64 mmol, 32 equiv.) were dissolved in acetone at room temperature under stirring, and epibromohydrin (EBH) (8.77g, 64 mmol, 32 equiv.) and 18-crown-6 as a phase-transfer (0.465 g, 1.76 mmol, 0.88 equiv.) as a phase-transfer catalyst (PTC) were added to the solution. The mixture was refluxed for four days with vigorously stirring. The reaction mixture was diluted with chloroform and washed three times with water. The chloroform solution was dried overnight with

anhydrous Na_2CO_3 and filtered. The chloroform was evaporated in vacuum, and a solid product precipitated from the methanol and was dried for 24 h in vacuum.

The product was characterized by $^1\text{H-NMR}$, IR and MALDI. $^1\text{H-NMR}$ (300 MHz, CDCl_3), 1.44 (d, , 3.0H), 2.40–3.05 (m,4.0H), 3.24–4.42 (m, 6.0H), 4.63 (m, 1.0 H), 5.80–6.75 ppm (m, 2.0H). IR (KBr): 2800-2950 (C-H stretch), 1600 (C=C of aromatic) 1465 (CH_2 bend) 1379 (CH_3 bend) 1140-1215 (C-O-C). MALDI spectrometry found signal at m/z 992.7.

3.6 Conclusion

Negative tone molecular resists based on Calix[4]resorcinarenes derivatives were synthesized to be investigated as future UV and e-beam curable material for lithography. Calix[4]resorcinarene (C4MR) was synthesized and fully functionalized by nucleophilic substitution reaction of the phenol in a presence of a phase transfer agent. The studied functional groups were oxetane, allyl and epoxide groups resulting in C4MR-8Ox, C4MR-8Allyl, and C4MR-8Ep. These synthesized compounds were characterized by ¹H-NMR, IR and MALDI.

Variable-temperature NMR of C4MR-8Allyl was studied. At room temperature, broad peaks were observed in aromatic, allyl and vinyl regions, which were attributed the presence of several conformers. However, at -70°C, NMR peaks in these regions became sharp. This is attributed to freezing bond rotations at low temperature, which restricts interchange between different conformers. Coalescence temperature was determined for aromatic and allyl regions based on the NMR spectra at different temperatures. The energy barrier of exchange (ΔG^\ddagger) was determined from coalescence temperatures to be 57.4 for the aromatic and vinyl hydrogens and 62.1 KJ/mol for the allylic hydrogens.

3.7 References

- (1) Oh, T.-H.; Ganesan, R.; Yoon, J.-M.; Kim, J.-B. *process of SPIE* **2006**, 6153, 61532G.
- (2) C. D. Gutsche In *Royal Society of Chemistry* Cambridge, England, **1989**.
- (3) Mandolini, L.; Ungaro, R. Imperial College Press:, London, **1999**.
- (4) Hennrich, G.; Murillo, M. T.; Prados, P.; Song, K.; Asselberghs, I.; Clays, K.; Persoons, A.; Benet-Buchholz, J.; de Mendoza, J. *Chemical communications* **2005**, 2747.
- (5) Ito, H.; Nakayama, T.; Sherwood, M.; Miller, D.; Ueda, M. *Chem. Mater* **2008**, 20, 341.
- (6) Fujita, J.; Onishi, Y.; Ochiai, Y.; Matsui, S. *Appl Phys Lett* **1996**, 68, 1297.
- (7) Nishikubo, T.; Kameyama, A.; Tsutui, K.; Iyo, M. *J Polym Sci Part A: Polym Chem.* **1999**, 37, 1805.
- (8) Iyo, M.; Tsutui, K.; Kameyama, A.; Nishikubo, T. *J Polym Sci Part A: Polym Chem.* **1999**, 37, 3071.
- (9) Nakayama, R.; Haba, O.; Ueda, M. *Polym Prepr Jpn.* **1998**, 417.
- (10) Gutsche, C. D. In *Calixarenes Revisited*; Royal Society of Chemistry: 1998.
- (11) Michael, A. *Am. Chem. J.* **1883**, 5, 338.
- (12) Niederl, J. B.; Vogel, H. J. *J. Am. Chem. Soc.* **1940**, 62, 2512.
- (13) Timmerman, P.; Verboom, W.; Reinhoudt, D. N. *Tetrahedron* **1996**, 52, 2663.
- (14) Niederl, J. B.; Vogel, H. J. *J. Am. Chem. Soc.* **1940**, 62, 2512.
- (15) Zinke, A.; Ziegler, E. *Berlin* **1944**, 77, 264.
- (16) Gutsche, C. D.; Dhawan, B.; No, K. H.; Muthukrishnan, R. *J. Am. Chem. Soc.* **1981**, 103, 3782.
- (17) Gutsche, C. D.; Dhawan, B.; No, K. H.; Muthukrishnan, R. *J. Am. Chem. Soc.* **1981**, 103, 3782.
- (18) Gutsche, C. D.; Dhawan, B.; Levine, E.; No, K. H.; Bauer, L. J. *Tetrahedron* **1983**, 39, 409.

- (19) Moore, D.; Watson, G. W.; Gunnlaugsson, T.; Matthews, S. E. *New Journal of Chemistry* **2008**, *32*, 994.
- (20) Tunstad, L. M.; Tucker, J. A.; Dalcanale, E.; Weiser, J.; Bryant, J. A.; Sherman, J. C.; Helgeson, R. C.; Knobler, C. B.; Cram, D. J. *J. Org. Chem.* **1989**, *54*, 1305.
- (21) Kondyurine, A.; Salzer, R. *Journal of Molecular Structure* **2001**, *563-564*, 503.
- (22) Matyjaszewski, K. New York: Marcel Dekker, Inc., **1996**.
- (23) Odian, G. *Principles of Polymerization* 4th ed ed. Hoboken, NJ: Wiley-Interscience., **2004**.
- (24) Lamanna, W. M.; Kessel, C. R.; Savu, P. M.; Cheburkov, Y.; Brinduse, S. *Proceedings of SPIE* **2002**, *4690*, 817.
- (25) Crivello, J. V.; Liu, S. *Journal of Polymer Science: Part A: Polymer Chemistry* **2000**, *38*, 389.
- (26) Crivello, J. V. *Polymer* **2005**, *46*, 12109.
- (27) Hassanein, E.; Higgins, C. *Proc. SPIE*, **2008**, *6921*, 692111.
- (28) Utomo, S. B.; et.al. *Indo. J. Chem.* **2011**, *11*, 1.
- (29) Senthamizh, S. R.; Nanthini, R.; Sukanyaa, G. *International Journal of Scientific & Technology Research* **2012**, *1*, 61.
- (30) Starks, C. M. *J. Am. Chem. Soc.* **1971**, *93*, 195.
- (31) Pavia, D. L.; Lampman, G. M. *Introduction to Spectroscopy* 2nd edition ed., **1996**.
- (32) Ammann, C.; Meier, P.; Merbach, A. *JOURNAL OF MAGNETIC RESONANCE* **1982**, *46*, 319.
- (33) Ogoshi, T.; Kitajima, K.; Umeda, K.; Hiramitsu, S.; Kanai, S.; Fujinami, S.; Yamagishi, T.-a.; Nakamoto, Y. *Tetrahedron* **2009**, *65*, 10644.
- (34) Günther, H. *NMR Spectroscopy*; Wiley, **1995**.
- (35) Denmark, S. E.; Forbes, D. C.; Hays, D. S.; DePue, J. S.; Wilde, R. G. *J. Org. Chem.* **1996**, *60*, 1391.

CHAPTER 4-SUMMARY AND FUTURE WORK

4.1 Summary

In this thesis, different molecular resists were either synthesized or examined in order to understand the relationship between their structures and properties. This allows for systematically designing resists with desired properties to achieve high resolution patterning performance.

In chapter 2, photoresist properties of different compounds with acrylate moiety were investigated. The main advantage of using acrylates was their high cross linking performance, which makes them a good choice as a negative tone photoresist. Furthermore, the curing process happened very fast for acrylates upon initiating radical polymerization. In this chapter, thermal curing of acrylate compounds in organic solvent was studied. Some issues were found with acrylate compounds that limits their use as resist compound such as shrinkage during crosslinking, and auto thermal polymerization. Auto thermal polymerization was observed in several studied compounds with different backbone and different number of acrylates. This is a major issue for using these compounds as resists. Based on the results of the acrylate study, the functional groups were switched to other crosslinking agents such as epoxy and oxetane.

In chapter 3, successful synthesis and characterization of calix[4]resorcinarenes (C4MR) and a series of full functionalized C4MR were reported. The functionalization was performed with oxetane, epoxy, and allyl groups. Figure 4.1 shows the structure of C4MR and the full functionalized compounds.

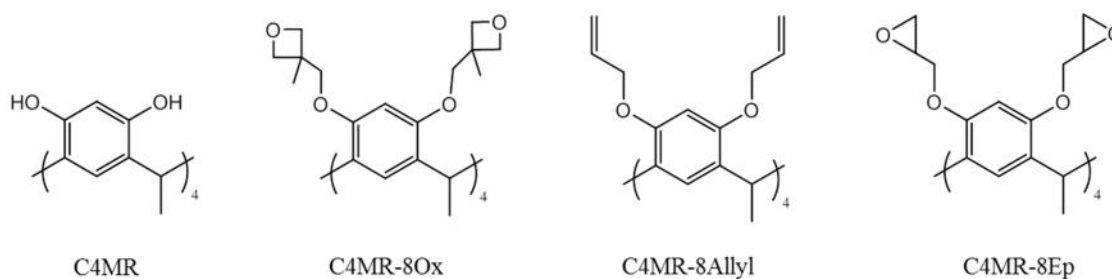


Figure 4.1. Structures of C4MR and full functionalized C4MR with oxetane (Ox), allyl, and epoxy (Ep)

C4MR-8Allyl shows interesting result in $^1\text{H-NMR}$ studies. At room temperature, broad peaks were observed in aromatic, vinyl, and allyl regions, which were attributed to the presence of several conformers. In order to further characterize the compound, NMR was studied at different temperatures. At -70°C , NMR peaks in aromatic, vinyl, and allyl regions became sharp. This might be due to freezing bond rotations at low temperature, which restricts interchange between different conformers. By using coalescence temperatures, energy barrier of exchange (ΔG^\ddagger) was calculated to be 57.43 for aromatic and vinyl hydrogens, and 62.14 KJ/mol for allyl hydrogens.

4.2 Future Work

As the semiconductor industry moves to smaller feature sizes, minimizing line edge roughness (LER), has become a major focus¹. Studies have shown that LER decreases with reduced molecular size²⁻³. Therefore, molecular glass is considered in order to decrease LER. Design of suitable structures is based on shapes that inhibit crystallization⁴, and have high glass transition temperature (T_g)⁵ such as C4MR derivatives. C4MR-8Ox and C4MR-8Ep were successfully synthesized as crosslinking

compounds for negative tone resist application. The future work is studying E-beam and DUV patterning performance of these compounds. Studying these compounds can result in a better understanding regarding the effect of different functional groups (oxetane and epoxide) on the patterning performance.

The next recommended future work is regarding the synthesis and characterization of partially functionalized C4MR, and studying their patterning performance. Presence of phenolic groups in the resist molecule may result in increased T_g, etch resistance, and base solubility. These fundamental concepts may guide future synthesis in half functionalized C4MR, to allow for the presence of phenolic group. Based on this strategy, synthesizing half functionalized C4MR with oxetane and epoxide groups is recommended.

These half functionalized compounds (C4MR-4Ox and C4MR-4Ep) can also be compared with full functionalized compounds (C4MR-8Ox and C4MR-8Ep) to better understand the effect of hydrogen bonding interactions and the number of cross linking groups on DUV and e-beam patterning performance.

4.2.1 Preliminary Result

Preliminary results were obtained in synthesizing half functionalized C4MR compounds. Half functionalized C4MR with oxetane (C4MR-4Ox) was synthesized along with other compounds in a mixture. The presence of C4MR-4Ox was confirmed with MALDI. Separation and further purification of C4MR-4Ox, as well as assessing patterning performance is recommended as a future work. The following is the synthesis procedure and characterization.

C4MR (2.99g, 5.5 mmol, 1 equiv.) and KOH (1.23g , 22 mmol, 4 equiv.) were mixed in DMSO at room temperature under stirring. After stirring for 30 minutes, 3-(chloromethyl)-3-methyloxetane (2.64g, 22 mmol, 4 equiv.) was added dropwise to the solution. The solution was stirred for 48h at 75°C. It was diluted with DCM, and then washed (extracted) with water three times. The solution was dried with MgSO₄, and subsequently filtered. The filtrate was rotovaped, and then excess water was added to remove traces of DMSO. The solution was left overnight to precipitate, and after filtration, brown solid powder (3.5 g) was obtained.

¹H-NMR shows there is a mixture of functionalized C4MR present in the product. MALDI indicates that we have at least five different functionalized compounds (3, 4, 5, 6, 7 functionalized C4MR). HPLC also confirms that a mixture of five compounds are present. Separating partially functionalized C4MR compounds will be a logical future path in this study.

4.3 References

- (1) Silva, A. D.; Lee, J.-K.; André, X.; Felix, N. M.; Cao, H. B.; Deng, H.; Ober, C. K. *Chem. Mater.* **2008**, *20*, 1606.
- (2) Rau, N.; Ogawa, T.; Neureuther, A.; Kubena, R.; Willson, G. *J. Vac. Sci. Technol., B.* **1998**, *16*, 3784.
- (3) Kadota, T.; Kageyama, H.; Wakaya, F.; Gamo, K.; Shirota, Y. *Materials Science and Engineering C.* **2001**, *16*, 91.
- (4) Alig, I.; Braun, D.; Langendorf, R.; Wirth, H. O.; Voigt, M. H.; Wendorff, J. *J. Mater. Chem.* **1998**, *8*, 847.
- (5) Ishikawa, W.; Inada, H.; Nakano, H.; Shirota, Y. *Chem. Lett.* **1991**, *10*, 1731.